Available online at www.sciencedirect.com

ScienceDirect

MATTER AND RADIATION AT EXTREMES

Matter and Radiation at Extremes 3 (2018) 165−187

www.journals.elsevier.com/matter-and-radiation-at-extremes

Review article

Unraveling the surface chemistry processes in lithiated and boronized plasma material interfaces under extreme conditions

P.S. Krstic [a,*], J.P. Allain [b], F.J. Dominguez-Gutierrez [a], F. Bedoya [c]

[a] *Institute for Advanced Computational Science, Stony Brook University, Stony Brook, NY 11794-5250, USA*
[b] *Department of Nuclear, Plasma and Radiological Engineering, University of Illinois, Urbana, IL 61801, USA*
[c] *Plasma Science and Fusion Center, Massachusetts Institute of Technology, Cambridge, MA, 02139, USA*

Received 30 October 2017; revised 5 January 2018; accepted 8 March 2018
Available online 31 May 2018

Abstract

The review of recent theoretical and experimental research on the complex surface chemistry processes that evolve from low-*Z* material conditioning on plasma-facing materials under extreme fusion plasma conditions is presented. A combination of multi-scale computational physics and chemistry modeling with real-time diagnosis of the plasma-material interface in tokamak fusion plasma edge is complemented by ex-vessel *in-situ* single-effect experimental facilities to unravel the evolving characteristics of low-*Z* components under irradiation. Effects of the lithium and boron coatings at carbon surfaces to the retention of deuterium and chemical sputtering of the plasma-facing surfaces are discussed in detail. The critical role of oxygen in the surface chemistry during hydrogen-fuel irradiation is found to drive the kinetics and dynamics of these surfaces as they interact with fusion edge plasma that ultimately could have profound effects on fusion plasma confinement behavior. Computational studies also extend in spatio-temporal scales not accessible by empirical means and therefore open the opportunity for a strategic approach at irradiation surface science studies that combined these powerful computational tools with in-vessel and ex-vessel *in-situ* diagnostics.

PACS codes: 28-52.-s; 52.40.Hf; 82.33.Xj; 73.22.-f

Keywords: Plasma-material interface; Retention; Sputtering; Lithium; Boron; Quantum-classical molecular dynamics; X-ray photoelectron spectroscopy; Material-analysis particle probe

1. Challenges of plasma-material interactions exposed to fusion plasmas

The interactions of a thermonuclear tokamak plasma and the bounding material surface are inherently extreme. Providing energy from nuclear fusion and in particular, confining magnetically hydrogen isotopes to sustain the reaction is one of the grand challenges of today. Energetic charged, excited, neutral and neutron particles interact with a material surface that is constantly evolving under extreme conditions of heat, pressure, radiation and stress. This dynamic interaction results in the combination of two disciplines: plasma physics and material-surface science, resulting in one of the most challenging areas of multidisciplinary science. Plasma-material interactions (PMI) have an important role in the operation of a fusion reactor due to the high particle flux and heat-flux from the fusion plasma resulting in damage of the plasma facing components (PFCs), limiting their lifetime while the sputtered material effecting cooling the core plasma. One consequence of complex plasma-material interactions is the effect on the plasma edge pedestal where steep gradients of density and temperature of the electrons in the plasma can be significantly affected by the impurity flux and the recycling of hydrogen fuel from the wall surface. The PMI has multiple spatio-temporal fundamental processes and synergies [1−5]

* Corresponding author.
E-mail address: predrag.krstic@stonybrook.edu (P.S. Krstic).

https://doi.org/10.1016/j.mre.2018.03.003

driven by both the plasma on one side of the interface and the material transformation on the other. A major goal in PMI science is to extend high-performance plasmas for very long durations and to integrate this performance with PFCs that can withstand high heat and particle fluxes while maintaining structural integrity and controlling retention of fusion fuel [6,7]. The nuclear fusion plasma-material interaction provides an environment where both the radiation and matter interaction are at extreme conditions. Extreme conditions are here defined as those that drive matter far from equilibrium and in some cases "very far" from equilibrium. For example, current fusion tokamak experimental devices with power extraction levels between a few MW/m^2 are for the former case and those above 25−50 MW/m^2 heat fluxes with radiation damage of several tens to hundreds of dpa (displacements per atom) for burning-plasma fusion reactors, are for the latter case. Among the most elusive technical challenges for the advancement of thermonuclear magnetic fusion energy is the predictive control of hydrogen recycling in the PFC materials as well as the management of erosion and defects induced by plasma particle and neutron irradiation and these effects on plasma confinement [8,9]. One of the critical knowledge gaps is an understanding of the changes in surface composition and chemistry at the atomic-to-nano spatio-temporal scales in the extreme conditions in tokamak fusion plasmas. The non-linear coupling of energetic particles and the material surfaces that continually evolve under the extreme conditions of a tokamak plasma makes it difficult to measure and let alone predict material behavior. By establishing an understanding of the plasma-material interaction one would ultimately begin to establish links to overall tokamak machine performance across both time and spatial scales combining real-time measurements in these extreme environments. The tools of which would include validating advanced computational PMI codes with well-diagnosed *in-situ* facilities and connecting these results to provide tendencies and qualitative behavior that can guide materials design and tokamak operation regimes. Although there has been historically a recognition of the importance of plasma-material interaction in fusion tokamaks, the majority of the work has been inherently Edisonian with very limited capability to capture the dynamic, evolving material surface.

Both low and high Z choices for plasma facing surfaces (PFS) in present tokamak fusion devices have significant performance issues [4,5,10,11]. PMI research in the National Spherical Torus Experiment (NSTX) and its Upgrade (NSTX-U) of the Princeton Plasma Physics Laboratory is focused on testing a variety of PFC candidate materials including low-Z coated graphite, high-Z materials (W, Mo) and liquid metals. Although carbon has been down selected as a viable future plasma-burning fusion reactor wall material [12], it remains the primary material component in most existing experimental tokamak devices. Therefore, devices that study unique plasma confinement regimes and boundary plasma effects such as the work in NSTX-U leverage the use of wall conditioning techniques as enabling technologies. The conditioning of plasma facing carbon components by lithium and boron is an important part of this research effort and it has led to the improved performance in fusion reactor experiments [13,14]. This has included numerous pioneering research efforts on complex PMI surface chemistry and physics validated in NSTX plasma regimes [6,7,15−20].

The combination of high-energy, high heat-flux and the complex evolution of material surfaces exposed to tokamak plasmas result in deciphering mechanisms under extreme conditions with sophisticated experimental and computational tools. The work of Allain and Krstic is to couple experimentally-validated multiscale theory and simulation, starting from mutually verifying quantum mechanical and classical atomistic computations to study the dynamics of the creation and evolution of the plasma material interface under irradiation by atoms and molecules at boronized carbon, lithiated carbon, boronized-lithiated carbon, with both solid and self-healing liquid metals (e.g. lithium). The time scale of most of the surface chemical and topology changes is in the picosecond to nanosecond range of the atomistic approaches. The goal of this review is to provide a bottom-up understanding of phenomenology and predictive tools necessary for successful design of the relevant laboratory experiments of plasma-particles retention, sputtering, reflection and morphological changes in extreme conditions, as well as the input parameters for the source and sink terms in appropriate nano-to-mesoscale modeling.

Conditioning of PFCs is an important enabling procedure for tokamak operation [14]. A major challenge for magnetic fusion devices generally is to extend high-performance plasmas for very long duration, and to integrate this high performance with PFCs that can withstand very high heat and particle fluxes while maintaining structural integrity with controllable retention of fusion fuel in a severe fusion reactor environment. Conditioning with boron and lithium has led to improved performance of a variety of experimental fusion machines [15,21]. In NSTX-U wall conditioning with boron was used to provide fuel density control and impurity reduction [15,16]. NSTX-U is comprised of mostly carbon-based PFCs (i.e., ATJ graphite tiles) as stated earlier. Traditionally boron has been applied to the first wall of magnetic confinement machines via plasma-enhanced chemical vapor deposition (PE-CVD), using mixture of a buffer gas (e.g. He) and a gas that contains B atoms (e.g. diborane (B_2H_6) or trimethylborane ($B[CH_3]_3$)) [22].

Recent work with lithium coatings evaporated on a variety of metallic and graphitic surfaces in over ten tokamak fusion machines around the world, has provided an evidence of the sensitive dependence of plasma behavior on lithiated plasma facing surfaces [23−25]. Thus, in NSTX, Li evaporation decreased the H-mode access power threshold, increased the stored energy and allowed longer plasma discharges when compared with plasma discharges without Li conditioning [21]. These improvements have been correlated to the reduction of impurities and with the reduction of fuel recycling with the formation of Li-O-D complexes [17]. In addition, He-glow discharge (He-GDC) approaches have also been used together with wall conditioning using B or Li depending on the desired performance conditions of NSTX plasmas [26]. In this work

dedicated He-GDC treatment of graphite surfaces prior to Li deposition resulted in a reduction of fuel particle transport from the far scrape-off-layer (SOL) reducing the particle source into the SOL and resulting in enhanced plasma performance. In this example, the complexity of He-induced collisional kinetics and surface chemistry evolution has introduced new questions about existing capabilities for prediction of PMI under irradiation-driven effects at the surface of complex Li or B-treated graphite surfaces in NSTX and more generally in mixed re-deposited materials in fusion devices. Although future plasma-burning reactors likely may not use graphite (i.e. graphite at high temperatures will retain high amounts of tritium and it will degrade under neutron irradiation), an understanding of the dynamic surface chemistry of low-Z materials is critical for high-duty cycle fusion reactor operation. In addition, with over 70% of existing experimental tokamak devices consisting of carbon PFCs, this review provides additional insights on fusion plasma-induced material mixing and irradiation-driven chemistry with important ramifications on fuel recycling and impurity emission. Furthermore, this review also serves as an important case study on development of advanced computational approaches combined with in-vessel PMI diagnosis (e.g. PMI measurements inside tokamak environments) and *in-situ* ex-vessel PMI experiments that mimic conditions in tokamaks. This review article is not intended to be exhaustive but rather delve deeply in the methodologies and approaches of the complex PMI in fusion tokamak devices reflected mostly in the author's recent work on the subject. This is the first review that addresses a critical issue for nuclear fusion and nuclear materials in general on the importance of surface chemistry under *extreme* conditions found in nuclear fusion devices. The point is that this material is targeted to a broader audience and one that may not be as familiar with nuclear fusion. This review is also the first to bring together both *in-situ* experiments in extreme environments and advanced computational modeling in the area of plasma-material interactions. This is significant given that due to the extreme conditions both the empirical and computational models are used collectively to provide a better understanding. This review outlines and delineates a research approach at closing significant technology gaps that has challenged the PMI fusion community.

Although graphite will not be the focus of plasma-burning reactors, the use of carbon-based materials is still being considered. Thus, there is an emergent work in nuclear fusion materials research, which is examining materials such as SiC and complex steels where carbon plays a significant role. In addition, advanced refractory alloy materials with ductile-strengthened precipitates will use carbon-based phases. Furthermore, the aspects of lithium and boron in the context of the first wall and extreme conditions are significant for reactors and therefore serve as an excellent platform to discuss PMI. The intention of this review, however, is beyond just nuclear fusion and to provide an example of how computational tools together with *in-situ* diagnostics can both elucidate complex physics under extreme matter and radiation interactions.

2. Challenges to surface chemistry and physics under extreme fusion conditions

As discussed earlier, one of the critical knowledge chasms in fusion PMI science is deciphering the complex coupling of edge plasma with materials surface evolution. The plasma-material interface is a dynamic, evolving, reconstituted region of material that is constantly eroded and re-deposited a million times over, rendering conventional approaches to surface science inadequate to provide a complete picture of the key mechanisms governing fusion PMI. The extreme conditions found in fusion tokamaks also result in limiting access to material characterization. Moreover, conventional post-mortem characterization of material samples exposed to fusion plasma campaigns in experimental devices consisting of thousands of plasma shots cannot completely capture the dynamic nature of the PMI. The methodology requires combining several complementary conventional and non-conventional approaches to provide a more rich, comprehensive and accurate understanding of surfaces under extreme fusion conditions.

For example, the characteristic fluence of D particles in low-*Z* covered surfaces can range from a few seconds to cumulative time of a few hours. Fluxes usually between few 10^{13} cm^{-2} s^{-1} up to 10^{21} cm^{-2} s^{-1} can drive matter very far from equilibrium whereby phase transformations along a surface yields irradiation-driven compositions that can change hydrogen retention by orders of magnitude. Moreover, the impurity retention and emission, and in particular the role of oxygen, could never be captured unless one is actively observing these variations during the timescale of modification (e.g. during plasma-induced modification time scales).

In this respect, specialized real-time PMI tools are designed and integrated into existing tokamak experimental devices such as NSTX [18,27] complemented by ex-vessel *in-situ* characterization facilities that mimic pre-determined conditions such as incident ion energy, species, angle and fluence coupled to surface characterization tools (e.g. X-ray photoelectron spectroscopy (XPS), low-energy ion spectroscopy (LEISS), thermal desorption spectroscopy (TDS), etc.). Although pure surface science platforms can in fact inform on fundamental aspects of material surfaces exposed to energetic particles found in non-equilibrium plasmas, they can only capture a limited aspect of the complex PMI under extreme conditions in tokamak plasmas. Furthermore, providing *in-situ* ex-vessel characterization facilities and approaches [28–31] is not sufficient and one must incorporate robust multi-scale computational tools that help elucidate and extend experimental measurements. This approach to fusion PMI is defined by “irradiation surface science” whereby one must bring the coupled PMI mechanisms under both computational and empirical approaches with sophisticated multi-scale tools that access states of matter (e.g. solid, plasma, gas) evolving over the course of irradiation-driven kinetics.

In the extreme environment encountered in fusion devices impurity control and hydrogen fuel management can become elusive. Since oxygen is always present in carbon, the

conditioning material, as well as from water ambient background, its concentration is greatly enhanced in the interface surface layers by deuterium irradiation, reaching over 20% atomic concentration in both lithiated (Fig. 1) [6], and boronized carbon (Fig. 2) [18]. Note that in Fig. 1(b) the oxygen concentration is decreased with deuterium irradiation (by chemical etch) and increased with deposition of Li. Therefore, complex computational tools require the inclusion of oxygen as an important component of the studied surfaces [2,14,32]. In the case lithium is present in the mixture of the plasma-material interface, the surface dynamics and chemistry is substantially changed, in comparison to hydrocarbons. Lithium, like other alkali metals, has a weakly bound valence electron. Lithium is the lightest of all metals, i.e. its low Z ($Z = 3$) implies two electrons strongly bound in a closed $1s^2$ shell, while the third electron is loosely bound in the open 2s shell, implying a large effective radius of the atom.

This may have consequences to the morphology of the materials containing lithium. However, the weak bonding also causes that the 2s electron is easily deformed in the vicinity of other atoms, extending the orbit toward these atoms, transferring partially or completely the quantal electron distribution to the neighbors, thus inducing electric charge interactions. Long range interactions in molecular dynamics have been readily "avoided" in the past because of the possible prohibitive computational cost. Namely, it is difficult to study the Li dynamics theoretically because of its polarizing features when interacting with other elements. These features are most transparently represented by the quantity called electronegativity, i.e. the chemical property of an element which defines its tendency to attract electrons. The electronegativity of Li is exceptionally low, and it is lower in comparison to that of the elements readily met in NSTX. On the other hand, oxygen has an exceptionally high electronegativity and it acts as a getter of negative charges in the material mix.

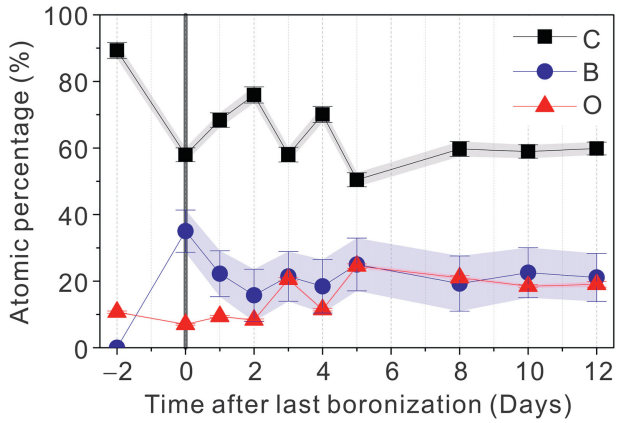

Fig. 2. Concentrations of O, B and C measured by XPS in the boronized ATJ graphite sample *in-situ* for increasing plasma exposure in the NSTX-U device. The shaded colored areas are ± one standard deviation about the mean values. *Figure reproduced from Ref.* [33] *with permission from the authors.*

The commonly accepted electronegativity scale is proposed by Pauling [34], and in that scale Li has an electronegativity of 0.98, carbon of 2.55, hydrogen 2.2, tungsten 2.36, molybdenum 2.16, boron 2.04, iron 1.83, tantalum 1.5, beryllium 1.57, and oxygen 3.44. Obviously, the very low electronegativity of lithium in comparison to the other fusion materials causes its positive polarization in mixtures with these materials, while the material becomes negatively charged (the whole system

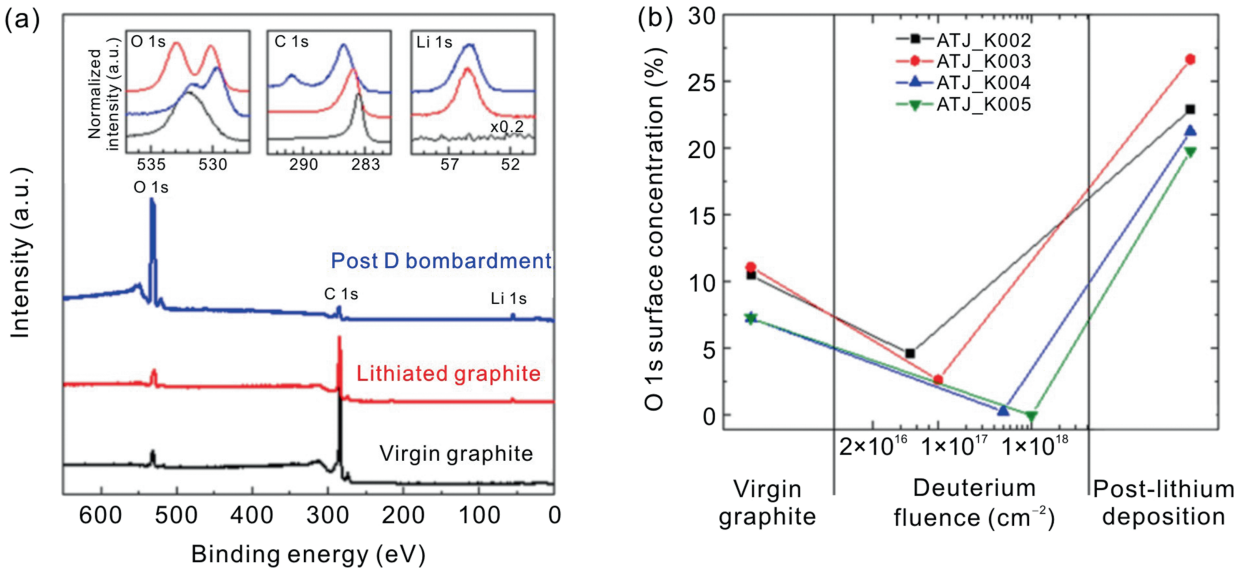

Fig. 1. (a) X-ray photoelectron spectra of lithiated graphite [5]. Un-treated virgin graphite (black) has two primary photoelectron peaks whose binding energies are characteristic of carbon C(1s) (~284 eV), and oxygen O(1s) (~532 eV) chemical bonds. Depositing lithium (red) on the virgin graphite results in the formation of a second peak in the O(1s) region (detail shown in O(1s) inset), which is indicative of new chemistry. Deuterium ion bombardment (blue) of lithiated graphite results in further induced chemistry in the O(1s) energy range as well as the formation of a new peak (i.e., new chemistry) observable in the C(1s) region (291.2 eV). The latter peaks represent deuterium-oxygen and deuterium-carbon bonds that are catalyzed by the presence of lithium on graphite. Furthermore, oxygen surface concentration of the lithiated graphite is greatly enhanced by deuterium bombardment. *Figure reproduced from Refs.* [17,20] *with permission from the authors.* (b) O 1s concentration on the virgin graphite, treated with 500 eV/amu D^+ for various fluences followed by exposure to Li deposition of about 1000 nm Li film post irradiation.

stays neutral). Particularly interesting is oxygen, which has exceptionally high electronegativity, giving its own contribution to the polarization of fusion materials. Since negative polarization of oxygen causes other fusion materials to become positively charged, thus opposing the effects of lithium, in case when both lithium and oxygen are present, typically Li and O strongly polarize each other while sign and strength of the polarization of other atoms in the mixture depends on the prevailing concentration as well as on volume or surface distributions of Li and O. Finally, when neither Li or oxygen are present in the mixture, similar electronegativities of the materials implies insignificant influence of the polarization properties. This opens the possibility for application of classical molecular dynamics with typical short-range interatomic potentials when studying the dynamics of such materials or material mixtures under irradiation of plasma. A possible exception are materials containing beryllium and/or tantalum, whose relatively low electronegativities might be a source of increased polarization features, especially if oxygen is present, a feature not yet studied in detail but that could have significant consequences for fusion-relevant materials such as beryllium used in ITER first wall and the ITER-like wall (ILW) experiments in JET [35,36]. In particular, these papers demonstrate the importance of materials mixing and how hydrogen retention is significantly affected in specific regions of the tokamak (e.g. in the inner-divertor region of JET-ILW).

The strong locally polarizing features of mixed materials containing lithium has important implications on the theoretical/computational and in particular, on atomistic approaches for treating the dynamics of these materials. Firstly, presence of electrically polarized atoms requires treatment of the long-range Coulomb and multipole forces, in addition to the short-range potentials usually used in molecular dynamics. This implies a large radius of interactions, and therefore a large number of atoms, n, which simultaneously interact. This can significantly increase the computational power requirements. Secondly, the polarizations, and therefore instantaneous charges of the interacting atoms and forces among them depend on coordinates of all atoms involved, i.e., they are functions of time in classical representation of atomic motion. However, classical dynamics is not capable of incurring these charge changes, since these are the quantum-mechanical effects of changes in the electron clouds of the atoms. This means that classical molecular dynamics *per se* is not a satisfactory approach to the dynamics of plasma-facing fusion materials containing lithium. The charges of the atoms that take part in the polar interactions depend on atomic coordinates, i.e., they change with time. The charges typically change in each simulation step. This narrows down the number of methods that can be used in studies of system dynamics to those that are capable of recalculating accurately the charges at each time step. If the classical molecular dynamics (CMD) is used, with pre-parameterized short-range potentials, a semi-empirical method like the Electronegativity Equalization Method (EEM) [37,38] has to be applied at each step (or after a small number of steps) for calculation of the atomic charges.

On the other hand, motion of the atoms as a whole is well described by classical mechanics at the temepratures of interest for fusion materials, since their quantum-mechanical, de Broglie, wavelength λ stays much smaller than the characteristic dimensions of both atoms and scale of their internuclear motion. For example, lithium atoms of kinetic energy 1 eV have a de Broglie wavelength of about 0.2 Bohr, which is much smaller than van der Vaals radius of the lithium atom (4.16 Bohr). In the case of a hydrogen atom, the de Broglie radius is about 0.5 Bohr, i.e. comparable to the atom radius, and one can expect some quantum mechanical oscillations in the 1 eV motion of the hydrogen atoms. However, due to the interactions with large number of atoms in the material, these oscillations may be averaged to a negligible effect. Only in very dilute materials, and at extremely low temperatures, the quantum effects of the atoms as a whole (i.e. their nuclei) may be of significant influence, which is not the case in plasma-facing fusion materials.

Thus, the interaction dynamics and chemistry in the fusion mixed materials containing lithium is well described by the so-called Quantum-Classical Molecular Dynamics (QCMD) [39,6], using quantum-mechanics to describe instantaneous motion of electrons in an instant of time of molecular dynamics, and then the resulting potentials to calculate forces that act to all atoms in the next time step. As a consequence of the partial charge transfer from Li to other atoms, the dominant long-distance binding force is the Coulomb attraction between opposite charges. Bondings between Li and other atoms are mixed covalent and polar. The differences in electronegativity between constituent atoms in Li−C, Li−O and Li−H systems are very large and therefore these systems could be considered as ionic solids.

The dynamic surface response and evolution in mixed material environments (with possible constituents D, Li, C, B, O) with impingement of plasma particles in the low energy range, including microstructure changes, erosion, surface chemistry, deuterium implantation and permeation have been extensively studied. The results based on the QCMD simulations and as well as by X-ray photoelectron spectroscopy (XPS) laboratory measurements [18,32,40,41] have demonstrated that increased oxygen content in the top carbon surface layers is the main driver for deuterium uptake in lithiated carbon surfaces. Thus, while the oxygen concentration in lithiated carbon surfaces is below 10%, it can reach over 30% upon sufficient irradiation by deuterium [32,40,41]. In this case lithium plays a role of catalyst, keeping the oxygen from degassing from the surface [32].

The plasma performance can be strongly influenced by the PFCs, which are modified with each exposure to the plasma. Critical to both an understanding and the practical operational strategy of tokamak PFCs with wall conditioning techniques is the role of surface chemistry over the entire plasma exposure. To establish this understanding both experiments and modeling have to be carefully planned and correlated and carried out as close as possible to the actual conditions in the tokamak to provide understanding of this synergistic relationship of the PFCs and plasma phenomena.

The computed deuterium retention probabilities of lithiated or boronized surfaces in various configurations were compared. Though both boronized and lithiated surfaces show similar trends in retention of deuterium when composition of the material is varied, the former surfaces show somewhat higher degree of retention, less dependent on the oxygen content than the latter surfaces. The experimental data [6,20,41] and new theoretical data [6,41] show a reasonable qualitative agreement for both lithiated and boronized surfaces [41]. Boron coatings on PFCs provide improved resistance to chemical sputtering and impurity retention thanks to a gettering effect associated with the formation of heavy oxides. However, erosion and passivation conjectured to be responsible for boron-associated improvements become only temporary and vanish after tens to hundreds of plasma shots [21]. The chemical sputtering of boron-doped graphite by hydrogen ions was studied experimentally by Chen et al. [42], though in the impact energy range of 700 eV to 3 keV. The chemical sputtering of boronized and oxidized ATJ carbon surfaces caused by deuterium impact was studied in range of 5−30 eV impact energy range.

Theoretical and experimental studies of sputtering of an amorphous carbon surface (a-C:D) have elucidated the chemical erosion mechanisms of carbon by hydrogen irradiation. This process does not require an energetic projectile and the ejected product is usually CD_x molecules [43−46]. Nevertheless, sputtering process is highly dependent of the surface parameters like temperature that can be elevated up to 1000 K [47,48]. Experimental studies of the temperature dependence of chemical sputtering of a-C:D by D were done by Mech et al. [46] and Balden et al. [49]. The discrepancy in both experimental data could be attributed to the experimental techniques and erosion measurements used by the authors. Theoretical methods based on Classical Molecular Dynamics (CMD) have been applied to study chemical erosion of a-C:D surface at different target temperature [50−52]. Numerical simulations were performed by Salonen et al. [50] to study chemical sputtering of a hydrogenated amorphous carbon surface in a surface temperature range of 300−1000 K. The authors conclude that the hydrogen concentration in the top of the surface reduces the carbon erosion and this effect could be observed in the experiment. CMD simulations have suggested that the decrease of the carbon erosion is not necessarily dependent of the hydrogen flux as reported experimentally, and external factors have to be considered such as redeposition or vapor shielding [51]. However, thermally induced stimulated processes of diffusion and desorption are important at target temperatures higher than 1000 K. These processes need longer time of simulation and CMD is not capable to model them [52].

Chemical sputtering measurements of plain and lithiated ATJ graphite have been performed at impact energies of 1−2 keV, showing that lithium deposition on ATJ graphite causes suppression of methane from the initial set of experiments reported in Ref. [53]. The authors report 69% of suppression of sputtered methane due to lithium coating on ATJ graphite at 453 K target temperature. It is interesting to note that deposited lithium on carbon does not form a layer, but it rather intercalates inside the carbon material. Sputtering yields on plane ATJ-graphite, pure lithium, and lithiated ATJ-graphite were measured at 500 eV/ion, 45° incidence, and sample temperatures of 25 °C and 200 °C. These experiments show that ejection of hydrocarbons is notably lower than that observed from a plane graphite [54]. In the NSTX, lithium sputtering yields from lithium-coated graphite plasma facing components increases as function of the temperature of the target [55]. A molecular dynamics study analyzed the effect of chemical sputtering of the lithiated, deuterated and oxidized carbon surfaces at 300 K by deuterium atoms in the impact energy range of 5−30 eV, which had not been studied before. The dependence of the sputtering process of the surface temperature in the range of 300−1000 K of a boronized and oxidized carbon surface by deuterium irradiation was also studied.

3. Methods for fusion extreme modeling and measurements

As discussed in Section 2, the distinctive feature of this research arises from the unique properties of lithium and oxygen, i.e., they easily charge in contact with other fusion materials, giving and getting partially or fully their external electron cloud to other atoms in its vicinity and polarizing the mixed material. Thus, quantum-classical molecular dynamics [6,39,56] is required in modeling of a lithiated, and possibly oxidized carbon surfaces because of the big differences in electronegativities of Li and C, O, B and D atoms. This causes long range Coulomb type interactions between the surface constituents, which depend on instantaneous coordinates of the atoms. QCMD can consistently treat the change of the electron cloud during the dynamics, but this requires an excessive computational time and resources. The quantum component of the QCMD solves the multi-electron eigenvalue problem at each time step of the system evolution, which could be computationally formidable problem even if Density-Functional Theory (DFT) is used. The use of approximations to DFT, like the Self-Consistent-Charge Tight Binding DFT (SCC-DFTB) method [57,58], makes the QCMD problem computationally feasible for study of deuterium retention or chemical sputtering at low energies (5 eV) [6,41]. Thus, in case of Ref. [6] a prepared cell was cut into rectangular box, with an approximate length of 1.5 nm, with a few hundreds of atoms, *x-y* periodic conditions were applied. The slab was bombarded by 5 eV D, perpendicular to the free cell interface, with 5004 random trajectories (needed for statistics) which were applied to each matrix-composition case, using embarrassing parallelization. Each trajectory was evolving at a separate node of Cray XT5, with the time step of 1 fs. About 6 h of CPU time was needed for most of the trajectories to finish their evolution, resulting either in reflection (the fastest), retention or sputtering (the slowest), thus requiring about 30,000 CPU hours per case. For 6 configurations in Ref. [6] this required about 200,000 CPU hours. If DFT was used rather than SCC-DFTB, this would require 100−1000 times

longer, which would be a formidable task, possibly feasible with future exa-scale computers.

Using in more recent times the Cray XK7 machine (Titan), and using improved version of the SCC-DFTB code, with use of GPU, the computation required 30 min for each trajectory (per node) with several hundreds of atom used. A minimum of 3000 trajectories used 3000 nodes of Cray XK7, i.e. about 1500 CPU hours per configuration. However, if we use this quantum-classical method in study of chemical sputtering in a range of energies 5–30 eV, this would become computationally too intensive, not only because the calculation has to be repeated for various energies, but also because higher energies require larger computational cells, as shown in Fig. 3, with inclusion of a larger number of active atoms. For 30 eV this means about $n = 2000$ atoms, and taking the scaling of SCC-DFTB with n as $n^{2.5}$, which would require about 200 times longer time. Repeating this computation for a number of impact energies and various configurations, this is becoming an exa-scale computational task.

These are the reasons the combination of CMD and electronegativity equalization method (EEM, [37,38]) could be the method of choice, for the sputtering studies. The latter is a semi-empirical method that applies a set of pre-calibrated, material and coordinate dependent parameters [13,14] to estimate change of charges of each atom as their coordinates change during the collision cascade of an impact atom in the surface. EEM is implemented [37] in the Large Scale Atomic/Molecular Massively Parallel Simulator (LAMMPS) [59] with Reactive Force Field method and potentials (ReaxFF), developed by van Duin and co-workers [60–62]. The EEM slows down computation by an order of magnitude, but this is still orders of magnitudes faster than QCMD, even when approximation to DFT is used for the quantum-mechanical component. On the other hand, ReaxFF is a bond-order potential, with proven capability to treat correctly chemical processes in the material of interest [60]. This approach was applied successfully in the previous work [41,63,64] to study deuterium retention and sputtering in boronized and lithiated carbon surfaces. When considering the impact energy range below the physical sputtering threshold, chemical sputtering is the main process of erosion. Consequently, one needs a good description of the deuterated, boronized or lithiated, and oxidized carbon surface (B(Li)-C-O:D) chemistry. The Bond Order Potential (BOP) of ReaxFF is well suited for this requirement. Verification of this approach to the BCOD chemistry by comparison with some of the relevant QCMD results shows good qualitative and even quantitative agreement [41].

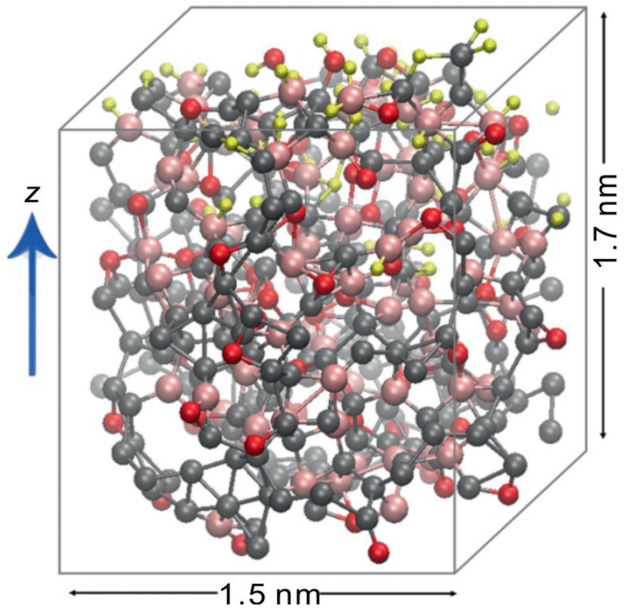

Fig. 3. Computational cell is a mixture of Li or B (pink) with C (gray) and oxygen (red), with accumulated D (yellow) atoms in the top surface layers upon bombardment with D. The z-axis is shown by the arrow. The periodicity is applied in x and y directions.

The range of the impact keV energies of the particles in ELMs is beyond the capabilities of the atomistic computational treatment based on QCMD, since this would require a much bigger computational cell due to the deeper penetration of the particles. However, classical MD, even with inclusion of EEM could be feasible for this task. Still, as discussed in Ref. [6], the retention happens at the end of the thermalization impact cascade, therefore its chemistry does not depend on the impact energy. What does depend on impact energy is the depth in the surface where the particles are retained, as well as configuration of the surface, i.e. the defects produced by energetic particles from ELMs. Still, one of the advantages of a liquid divertor (of Li, for example) idea is in removing the cumulative defects.

To decouple the complex extreme conditions found in fusion PMI simulations with state-of-the art in-situ experimental PMI the measurements are combined by Allain et al. including the so-called in-vessel diagnostics such as the Materials Analysis Particle Probe (MAPP) [18,65] shown in Fig. 4. This diagnostic is capable of *in situ ex tempore* (e.g. in between plasma shots) analysis of samples in the NSTX-U divertor region. The experimental X-ray Photoelectron Spectroscopy (XPS) measurements of the Boron-Carbon system, presented here, were obtained using MAPP during the NSTX-U FY16 experimental campaign [18]. MAPP is capable of performing surface diagnosis between plasma discharges of up to four samples that are inserted flush with the tiles of outboard divertor. This experimental approach allows us to obtain insights of the evolution of surface chemistry at the time scale of surface modification exposed to tokamak plasmas, since the samples can be retracted to an analysis chamber shortly after their plasma exposure. Other approaches include techniques to passively measure PMI events as well as ex-vessel characterization of samples conducted post-mortem [29]. The subtle interplay of boron, lithium, carbon, oxygen and deuterium chemistry is explained by QCMD and reactive molecular dynamics simulations, verified by quantum-classical molecular dynamics and successfully compared to the measured XPS data provided by MAPP in the case of the B-C-D complex. In this context, the off-line *in-situ* experimental facilities which can carefully mimic some of the

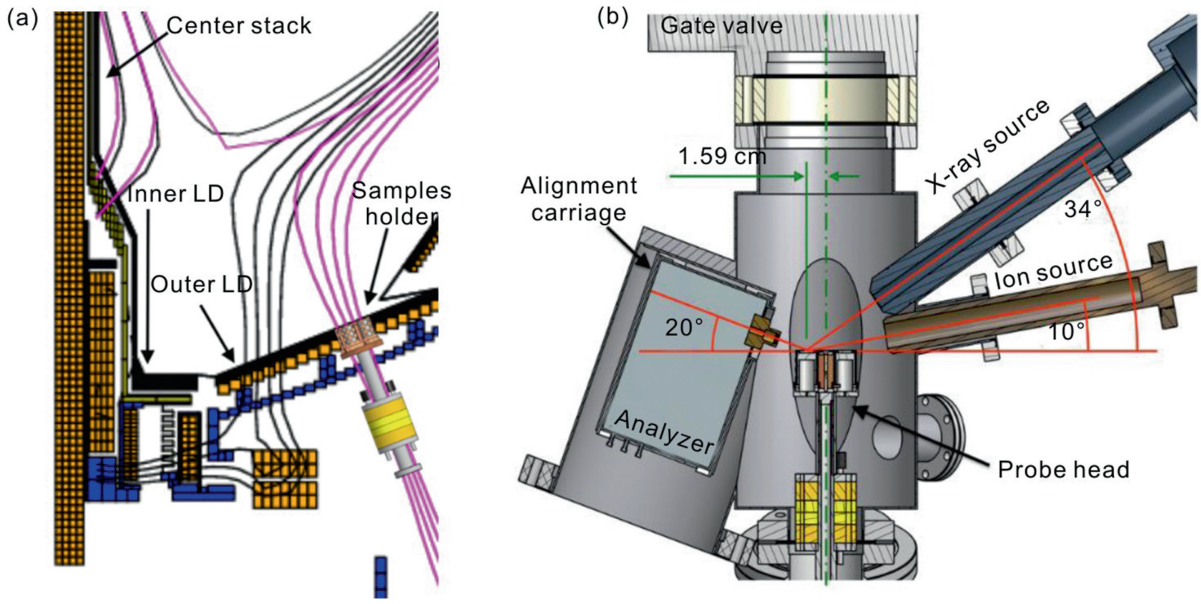

Fig. 4. MAPP samples holder in the inserted position in NSTX-U. The samples are exposed to the same conditions as the PFC in the outer divertor of the tokamak, this position is shown in (a). The sample holder can be retracted in between plasma discharges to a custom designed analysis chamber for XPS measurements, the analysis chamber is shown in (b). *Figure reproduced from Refs.* [15,66] *with permission from the authors.*

important conditions found in tokamak edge plasmas and their interaction with candidate material surfaces can validate these codes [28].

The ATJ graphite PFCs in NSTX-U are boronized by a glow discharge with 95% He and 5% deuterated trimethylborane (d-TMB, $B(CD_3)_3$) followed by 2 h of He Glow Discharge Cleaning (He-GDC) that depletes deuterium from the surface [10]. The NSTX-U PFCs were exposed to deuterium plasmas with a cumulative daily duration up to 36 s and 8 min of intershot He-GDC [11]. Deuterium also outgasses from the PFCs in the intervals between plasmas. XPS measurements are reported at the end of each day after exposure of the MAPP sample to deuterium plasmas. They thus represent the cumulative effect of plasma exposure and between-shot He-GDC. They discriminate, however, against the outgassing between the run days.

4. Understanding PMI in extreme conditions

Detailed recent studies are presented in this section of deuterium retention and sputtering of 1) boronized, oxidized and deuterated carbon surfaces, and 2) lithiated, oxidized and deuterated carbon surfaces.

4.1. Retention

4.1.1. The effect of D irradiation on oxygen surface concentration in lithiated graphite

XPS *in-situ* experiments by Taylor and Allain have confirmed that the positive features of the lithium coating are connected somehow to larger concentrations of oxygen on the surface (Fig. 1). For example, in various samples an average of 6% of oxygen was measured at the virgin graphite surface, which then increased to an average of ~10% after lithium conditioning of the ATJ graphite surfaces. Bombardment with the low-energy deuterium, however, elevated the content of oxygen in the near-surface interface to more than 25%, and even exceeding 45% in the zone of interface for various samples (Fig. 5). This unexpected experimental finding, combined by the understanding of morphology of the lithiated carbon surface, was motivated by the computational simulations of Krstic et al. and transformed the fusion community understanding on the deuterium retention mechanism in the lithium-based surfaces. Rapid intercalation and micrometer surface morphology prevent the lithium from acting as a surface layer, but rather looks like lithium seeping into mountainous carbon (Fig. 6).

Deuterium bombardment results in additional irradiation-enhanced chemical processes which are visible in both the O(1s) and C(1s) photoelectron ranges from XPS data (see Fig. 1). These resultant Li-O-D and Li-C-D interactions only appear when exposing lithiated graphite to deuterium bombardment. These analyses exploit an indirect method of observing deuterium interactions on lithiated graphite since deuterium atoms do not emit photoelectrons sufficient to be detected via XPS. The dramatic increase in surface oxygen content in Fig. 5 during deuterium bombardment is astounding when considering that previously, oxygen was not even considered to contribute in retaining deuterium.

4.1.2. The importance of oxygen surface concentration levels for D retention chemistry with lithiated graphite

Initially, researchers supposed that deuterium is retained in lithiated graphite via a direct lithium-deuterium interaction, resulting in the formation of lithium deuteride (LiD) [67,68]. This conjecture was supported by experiments with pure lithium surfaces. For example, deuterium ion beam and plasma discharge experiments with liquid lithium showed that liquid

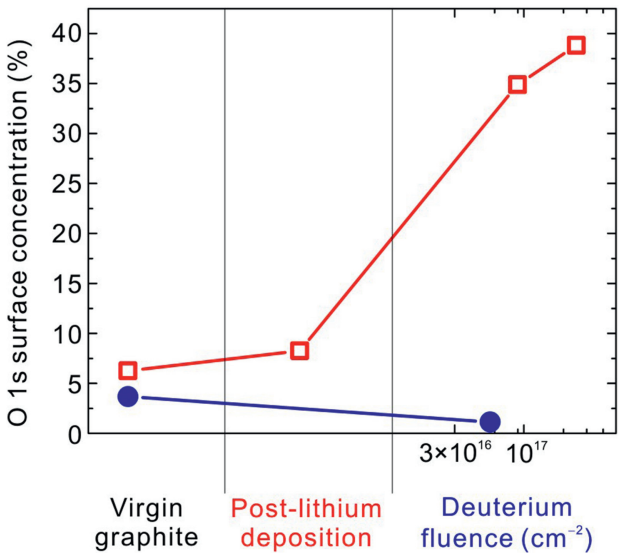

Fig. 5. Oxygen evolution during irradiation. This figure illustrates that lithium conditioning of graphite increases the surface oxygen content and that ion bombardment accelerates the increase. Polished ATJ graphite has an average oxygen surface concentration of 6.3% as measured by XPS. In samples represented by the hollow red squares, lithium deposition increases the surface oxygen content to ~8%. However, deuterium ion irradiation of the sample greatly enhances the oxygen content to more than 35%. In stark contrast, irradiating a sample without lithium conditioning (blue filled circled) actually decreases the amount of oxygen on the surface to 1.1%. *Figure reproduced from Refs.* [17,20] *with permission from the authors.*

lithium could retain deuterium at ratios as high as 1:1 [69,70]. Lithiated graphite, however, incorporates completely different physics. One challenge is that the deposited lithium coating intercalates (diffuses) into the graphitic tile, down to about 2–3 μm [68] and thus questions arise regarding how the mixture of lithium and carbon atoms is able to retain deuterium so effectively. This is particularly true due to the complex covalent bonding character of the Li-C-O-D system compared to the well-known ionic bonding in the LiD salt. Direct LiD bonding in graphite is unlikely since it would require that the lithium freely sit on the surface waiting until a deuterium ion arrives to bind. For impermeable substrates where layers of "pure" lithium accumulate, direct LiD bonding may be feasible, but lithium-graphite intercalation further precludes this from occurring [7,69,70]. Lithium's ability for absorbing oxygen from the ambient environment (e.g. oxygen from walls, water and lithium evaporant) casts doubt on the validity of the formation of pre-dominant LiD bonds in lithiated graphite. In fact, the surface analysis conducted by Taylor et al. showed that lithium began to interact with carbon and oxygen immediately upon deposition [7,71].

The first attempt to describe deuterium retention in lithiated graphite used an atomistic modeling in a Li-O-C-D matrix, and generated a reasonable conjecture on possible mechanisms for the retention of D in lithiated graphite [56]. The electropositive nature of Li and its interaction with the majority of atomic elements suggested that lithium readily binds less electropositive hydrogen and carbon [34]. Thus, the initial simulation included only a modest 5% O atoms (typical for industrial graphite), 23% Li atoms, and the balance filled by C atoms. This composition led to a preference of H for interacting with Li rather than with C, with a minor role being played by O corresponding to its small percentage. However, XPS data clearly showed significant variations in surface chemistry that were directly attributed to the O(1s) peak and only in the presence of lithium [7]. Furthermore, these changes were directly correlated to fluence-dependent D irradiations [71]. The resultant Li-O-D and Li-C-D interactions only

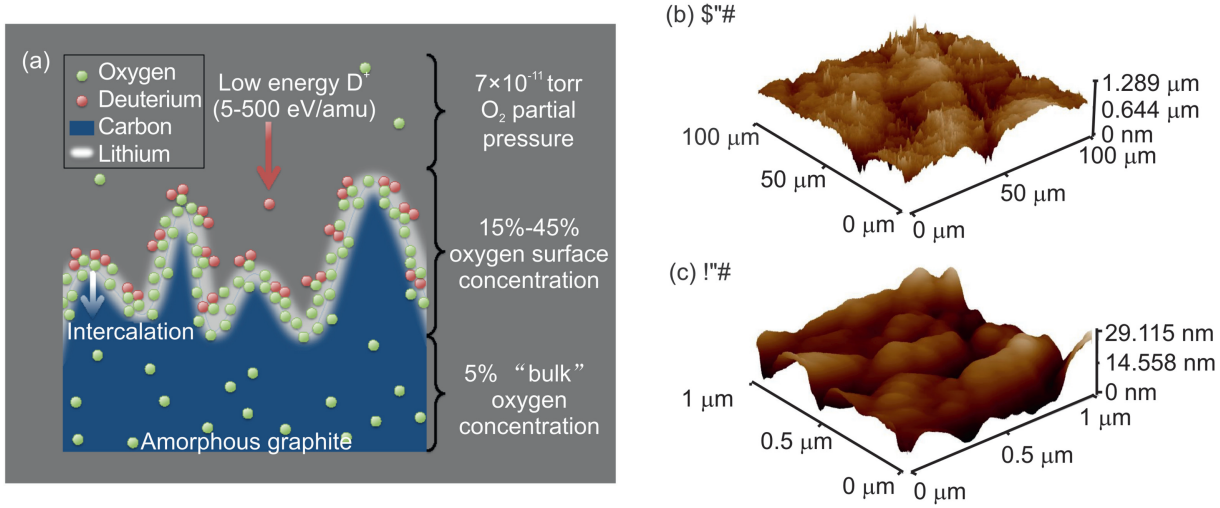

Fig. 6. Illustration of the dynamics in lithiated graphite. Polished graphite samples have surface height variations of >1 μm (for a 100 μm × 100 μm domain) in addition to local height variations on smaller domains, as shown in the inset atomic force micrographs (AFM) in (b) and (c). When depositing lithium films on such rough surfaces, the effective film "thickness" is significantly less than the nominal dose due to the increased effective surface area. Furthermore, lithium rapidly intercalates into graphite following deposition. Highly electropositive lithium attracts electronegative oxygen from the polished graphite (~6% O_2 concentration) as well as from the ambient vacuum (O_2 partial pressure of ~10^{-11} torr during lithium deposition). Lithium deposition *per se* causes a modest average rise in surface oxygen content to approximately 10%. However, for some samples, experiments show that deuterium ion bombardment dramatically increases the surface oxygen content to as much as 45%. *Figure reproduced from Refs.* [17,20] *with permission from the authors.*

appear when exposing lithiated graphite to deuterium bombardment. Finally, the computer simulations [6] reached qualitative agreement with experiments, showed that an elevated oxygen concentration was a missing ingredient in the previous [56] simulation studies. This was the first time that complex quantum atomistic simulations were used to complement *in-situ* experiments deciphering the dynamic chemistry and physics of surfaces exposed to the extreme environment of a tokamak edge plasma.

A simulation cell of a few hundred atoms of lithiated, oxidized and hydrogenated amorphous carbon (a-C), at 300 K, was used in [6] and bombarded with five thousand random trajectories using QCMD, to determine the final rest location of the projectile deuterium in relationship to other elements in the matrix, it is a qualitative method used to determine likely binding pairs in Fig. 7. An identical deuterium bombardment sequence was conducted in five different matrices as indicated in Fig. 7: Matrix A: 100% amorphous carbon (panes a-b); Matrix B: 80% amorphous carbon, 20% lithium (c-d); Matrix C: 60% amorphous carbon, 20% lithium, 20% oxygen (e-f); Matrix D: 52% amorphous carbon, 16% lithium, 16% oxygen, 16% hydrogen (g-h); and Matrix E: 80% amorphous carbon, 20% oxygen (i-j).

In Fig. 7(c−d) where the sample contains 20% lithium, less than 10% of deuterium finds lithium as its nearest neighbor. However, when the sample is loaded with 20% oxygen (Fig. 7(i−j)), over 30% of deuterium finds oxygen as its nearest neighbor. The case where the carbon matrix contains 20% lithium and oxygen (Fig. 7(e−f)) also shows that deuterium has ~30% oxygen as its nearest neighbor with minimal lithium nearest neighbors. Thus, even when lithium is present in the carbon matrix, deuterium preferentially chooses the vicinity of oxygen for its final bonding. Another qualitative method for determining binding pairs comes by analyzing the charge distribution of the matrix constituents. Likely binding pairs are identified as a negatively charged atom is neutralized by a positively charged counterpart. The charge distributions of all elements for the same compositions A-E are shown in Fig. 8, in full agreement with the findings in Fig. 7, indicating that lithium is not playing the major role in retaining deuterium if there is a comparable or higher concentration of oxygen. This is also consistent with the recent first principles computational chemistry calculations [72,73] using Plane-Wave DFT on binding chemistry of H, O and Li in the graphene matrix. Oxygen neutralizes ~25%, carbon neutralizes ~68% of the deuterium, and lithium is responsible for ~7% deuterium neutralization, as seen from Fig. 7(e).

4.1.3. Deuterium retention chemistry and impact energy

An apparent "gap" between the model calculations and the experimental data in the impact energy of D was the limitation introduced by the simulation cell. Previous studies of plasma-carbon surface interactions that led to very successful quantitative agreement between atomistic simulations and experiments were based, in fact, on the ability to "mimic" the experiments as close as possible [44]. In the studies presented in this subsection, experiments were conducted at incident deuterium energies between 25 and 500 eV/amu. However, the

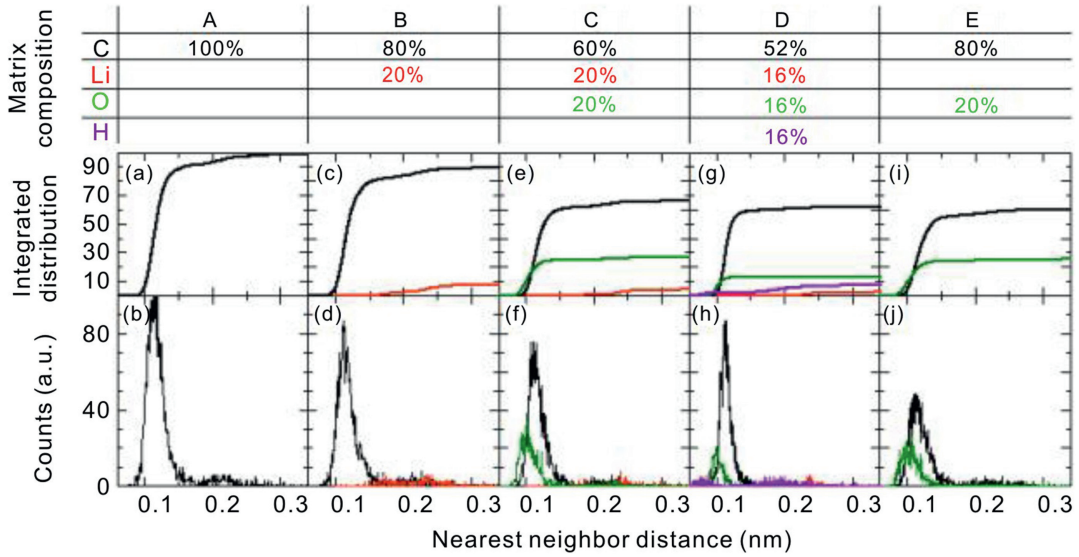

Fig. 7. Distribution of nearest neighbors. Calculation of the final rest location of the projectile deuterium in relationship to other elements in the matrix was performed with five thousands random trajectories per matrix. The distance (horizontal axis) of nearest neighbor species to retained deuterium, within the simulation matrix following D-atom bombardment, is used to indicate the frequency of elemental binding pairs. The deuterium bombardment was conducted in the five different matrix compositions A, B, C, D, and E. The distances from deuterium to carbon are shown in black, to lithium in red, to oxygen in green, and to sample-preloaded deuterium in purple. The top panes represent the integrated distributions of the nearest neighbors, shown in the bottom panes. Even when there is an equal quantity of O and Li in the carbon, as seen in case C, Fig. 7(e−f), the oxygen by far dominates as the nearest bonding neighbor where >20% of the implanted deuterium ions have oxygen as their closest neighbor and <5% have lithium. In case E, Fig. 7(i−j), where the carbon matrix is void of lithium and has 20% of oxygen, implanted deuterium atoms are still 30% of oxygen as closest neighbors, indicating more than one D atom bonding to one O atom. Importantly, if added a "cumulated" deuterium so that Li, O and D have the same, 16%, atomic fraction in carbon, case D, the qualitative conclusions drawn from other cases in Fig. 7 are still valid, as can be seen in (g−h).

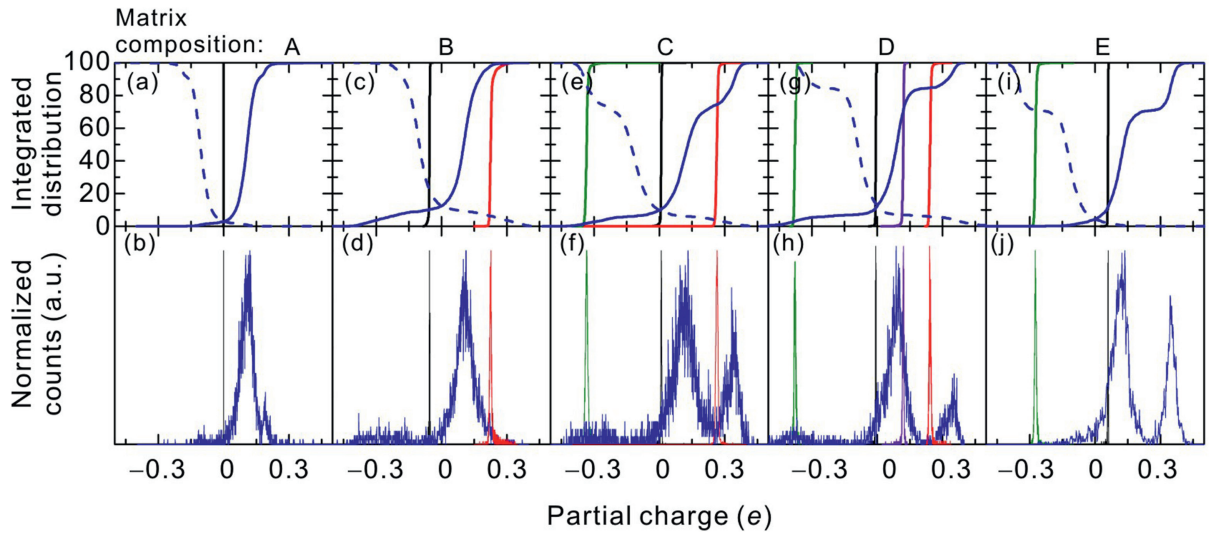

Fig. 8. Distribution of charges following D bombardment by 5000 independent random trajectories. The top panes represent the normalized integrated distribution of charges shown in the bottom panes. The species charge distribution within the simulation matrix following deuterium ion bombardment is used to easily identify the strength of the elemental binding pairs. Contributions from carbon are shown in black, lithium in red, oxygen in green, sample-preloaded with hydrogen in purple, and impacting deuterium in blue. Above, deuterium bombardment was conducted on five different matrix compositions (Fig. 3 in the text). Matrix A: 100% carbon (panes a–b); Matrix B: 80% carbon, 20% lithium (c–d); Matrix C: 60% carbon, 20% lithium, 20% oxygen (e–f); Matrix D: 52% carbon, 16% lithium, 16% oxygen, 16% hydrogen (g–h); and Matrix E: 80% carbon, 20% oxygen (i–j). In the bottom panes, binding pairs are approximately polarized about 0.0 *e*. For convenience in showing what species neutralizes deuterium, the deuterium-integrated distribution is also shown flipped (dashed lines) with its flipped sign. Thus in (f) oxygen at −0.33 *e* (*e* is an elementary charge) is neutralizing the deuterium at +0.34 *e*, lithium at +0.26 *e* neutralizes the small deuterium peak at −0.26 *e*, and the remaining deuterium at +0.1 *e* is counterpoised by the highly neutral carbon. (e–f) quantitatively shows the neutralizing effect of each species.

quantum-classical simulations were limited to simulation cells not larger than a few hundred atoms, resulting in maximum penetration depths of about 1 nm, and therefore impacting deuterium energies of about 5 eV. Since most of the chemistry between deuterium and the surface happens at the end of the D-induced impact cascade, when the D atom is almost thermalized with the other atoms in the surface, it was expected that the impact energy would have no effect on the qualitative conclusions of the deuterium chemistry. Two independent experiments with XPS diagnostics were performed in bombarding lithiated ATJ graphite by deuterium at 200 eV and 50 eV [6]. As can be seen in Fig. 9, the binding energies of detected photoelectrons are constant regardless of the deuterium ion energy, which confirms that the in-surface chemistry qualitatively does not depend on the impact energy.

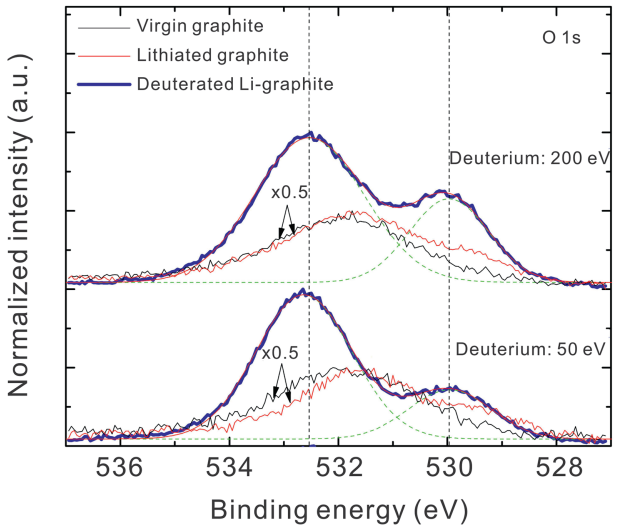

Fig. 9. Chemistry occurs at ion end-of-range. Energetic deuterium ions slow down to thermal energies after entering the lithiated graphite substrate. Chemistry occurs at the end-of-range for the ions. The XPS data here (blue traces) show lithiated graphite bombarded by 50 eV and 200 eV deuterium ions with nominally identical results. The peak at ~530 eV represents Li-O bonds and the peak at ~533 eV represents D-O interactions catalyzed by lithium. *Figure reproduced from Ref.* [6] *with permission from the authors.*

4.1.4. Discussion on the D retention in lithium

From the collection of both experiments and computational modeling the primary mechanisms responsible for retention of deuterium in lithiated graphite can be now summarized. First, experiments [7] showed that deuterium retention occurs via mechanisms that include O and C, not simply Li-D. Next, computational modeling results contended that deuterium is primarily bound by oxygen in the Li-C-O matrix. Subsequent experiments showed that once the lithiated graphite (with only ~10% oxygen on the top 4–8 nm) is irradiated with deuterium, the concentration of oxygen in the top < 10 nm can increase dramatically to as much as 45%. There is an associated effect of irradiation-enhanced oxygen gettering (i.e., from residual oxygen-containing gas in the vacuum) and irradiation-induced oxygen segregation to the surface playing important roles. However, what is the role that lithium plays in this process? The key point is that lithium is a physical catalyst that brings oxygen into the surface (e.g. either from residual gases, breakup of water, or Li-O in the sub-surface promoted to the surface from the bulk by irradiation) thus increasing the probability of D retention by oxygen atoms. ATJ graphite is

mostly amorphous in fusion devices such as NSTX and the morphology plays a vital role in D uptake. Lithium, although being partially ionized (typically +0.3*e*, Fig. 8) in the carbon environment has covalent radius significantly larger than carbon, expands the amorphous graphite region providing pathways that when irradiated with D will promote oxygen segregation (predominantly with Li-O) to the surface. This tendency will therefore grow with two factors: 1) the amount of lithium in ATJ graphite and 2) the D fluence that drives the oxygen via Li-O bonds to the surface for the same amount of lithium in graphite. Therefore, it is the *inherent* extreme conditions of irradiated lithium-oxygen-carbon complex that drives D retention at these interfaces during D plasma irradiation. In fact, one may conjecture that the Li-O-D complex may in fact be also dependent on the time rate of change of D irradiation, e.g. the flux of D ions arriving at the surface. This is yet another finding that several experiments in high heat-flux plasma exposures demonstrated in the work by Taylor et al., Allain et al. and Neff et al. [74–76].

Fig. 10 presents the calculated retention and reflection probabilities (a) and sputtering yields of various surfaces upon impact of 5 eV D (b). As one would expect from the results in Fig. 10, Li does not do much to suppress sputtering or enhance deuterium retention, in fact, Matrix B with 20% Li and 80% C shows higher sputtering than the other compositions in consideration. It is the presence of oxygen, with or without lithium, which suppresses sputtering and enhances deuterium retention. This conclusion is consistent for single D bombardments as well as the case where deuterium "accumulates" in the sample.

These findings, consistent with the XPS data, have far reaching consequences: It is not lithium that suppresses erosion of C, and increases retention of H as conjectured by Yagi et al. [55]. Instead, oxygen plays the key role in binding of hydrogen, while lithium is the catalyzer for oxygen accumulation in the surface, i.e. lithium is the oxygen getter. When there is a significant amount of oxygen in the surface (e.g., ~4 times greater than in a non-lithiated graphite sample), it becomes the main player. This is true even when there is a comparable amount of lithium in the surface. Lithium has a minor direct influence on the deuterium uptake chemistry in carbon; however, in practice, lithium is essential in attracting the oxygen, which in turn retains deuterium. These conclusions are consistent with those of decades of laboratory and reactor-based experiments.

4.1.5. Surface chemistry in a boronized-carbon surface

The study was performed of the role of boron and oxygen in the chemistry of deuterium retention in boronized ATJ graphite irradiated by the extreme environment of a tokamak deuterium plasma. The reactive classical molecular dynamics simulations, enriched by EEM, verified by quantum-classical molecular dynamics calculations provide understanding of the chemistry dynamics in the C, B, O, D quaternary surfaces, irradiated by D for various deuterium concentrations. The role of oxygen and boron in the retention of deuterium is decoded, leading to the predictions similar to the results for the lithiated and oxidized

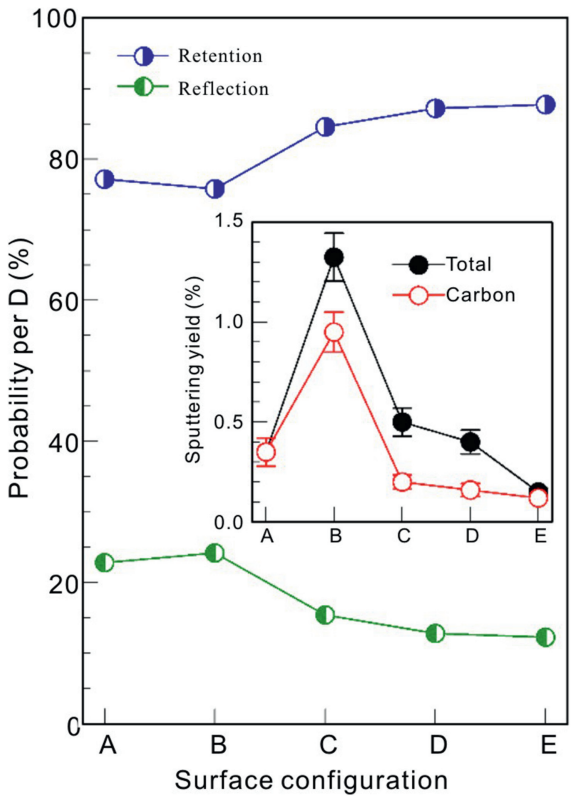

Fig. 10. Simulation results of D-retention and sputtering [6]. (a) Retention and reflection probabilities of impact D, and (b) total and C sputtering yields of the various cases, A-E, defined in Fig. 7. Presence of only lithium (case B) does not improve deuterium retention and carbon sputtering in comparison to the pure carbon (case A), it has a negative effect. When oxygen is present in amounts comparable to that of lithium (cases C, D, and E), positive effects to the deuterium recycling and carbon erosion are apparent. Deuteration of the carbon (case D) weakly influences this conclusion.

carbon surface. The simulation results were validated by in-situ ex-tempore XPS measurements, using MAPP inside the NSTX-U divertor chamber, to measure the effects of low energy deuterium irradiation of a boronized graphite.

The initially negligible role of oxygen to bond D in the BCO (<5% of D is bonded to O) is significantly increased (to almost 20%) by D uptake, which is in contrast to the role of oxygen in the D retention of LiCO surfaces [6]. It is well known that increased amounts of Li-based conditioning in high-triangularity plasmas in NSTX have demonstrated evidence of improved plasma conditions and D retention that exceed conditioning with boronization [10]. The unique role that oxygen plays in both lithium-treated and boron-treated graphitic surfaces and how ultimately their interface influence plasma performance is an on-going topic of research and beyond the scope of the work here. Nevertheless, combining the computational multi-scale tools presented here with *in-situ* PMI diagnostics are helping make links to plasma-induced effects on the edge and core.

The bonding in % of O-B, O-C, and O-B-D, illustrated by lines with symbols in Fig. 11(a) fall well in the uncertainty bands in the XPS spectra from O1s, were obtained averaging the concentrations of two consecutive days of the XPS data.

The calculated data are normalized to the total of atom bonds of the particular type. For example, in Fig. 11(a) the numbers of O-B, O-C and O-D bonds compare to the total number of oxygen bonds in the top 0.75 nm of the computational cell. The D concentration following the XPS spectra is likely due to the plasma-enhanced deposition of boron films supplying deuterium from the gas phase during the molecular dissociation, and thus, the time dependent effects of the D accumulation are not well described by these experiment. The D concentration is uncertain and decreases in time, because of the He-GDC and outgassing at the end of each day.

The colored bands from the XPS measurements and computed C-C, C-O and C-B curves in Fig. 11(b) are also well in agreement. There are, however, deviations in the B1s spectra for the B-C and B-O bonds of the measured and computed sets of values. Obvious asymmetry exists between C-B in C1s and B-C in B1s spectra. In Fig. 11(c) inconsistencies between C and O bands and calculated values indicate that "exposure" time of the deuterium irradiation might be responsible for the increased content of oxygen in the surface layers, the effect that cannot be "caught" by the short time scale of atomistic simulations. Consistent with such effect are calculations with 40% oxygen at the surface, shown by hollow symbols at Fig. 11. A similar mechanism for driving oxygen to the surface by D irradiation was found in lithiated graphite [6,7]. However, analysis of the calculated D retention chemistry in the inset of Fig. 12 shows that the role of O in bonding of D increases significantly with increase of D concentration, in contrast to the high role of oxygen in D retention for all D concentrations on the LiCO surface [6].

In this work, *in-situ* measurements combined with computer simulations of the surface chemistry in the plasma-facing materials exposed to the extreme conditions of tokamak plasma were executed for the first time inside NSTX-U, using MAPP. Significantly, the findings unravel critical role of oxygen and other impurities in the material retention chemistry. The details are presented in Ref. [33].

Fig. 12 shows the results of atomistic simulations, combining CMD-REAXFF and QCMD-SCC-DFTB, to obtain retention of deuterium and sputtering (Fig. 10) of lithiated or boronized and oxidized amorphous carbon surfaces exposed to the 5 eV deuterium impacts. The experimental and theoretical data show a reasonable qualitative agreement for both lithiated and boronized surfaces. Using the computational simulations we compare the deuterium retention probabilities and chemical sputtering yields of lithiated or boronized surfaces in various configurations. Though both boronized and lithiated surfaces show similar trends in retention of deuterium when composition of the material is varied, the boronized surfaces show somewhat higher degree of retention, less dependent on the oxygen content than the lithiated surfaces. Interestingly, the results in Fig. 13 for BCO mixture are quite different from those obtained for LiCO mixture in Figs. 7 and 8 [6]. Namely, while in case of LiCO the main role in bonding of D is played by oxygen, here bonding of D is dominated by boron. Boron is more reactive than oxygen because of the so-called octet rule, i.e. a coordination number of four is preferred for B atoms,

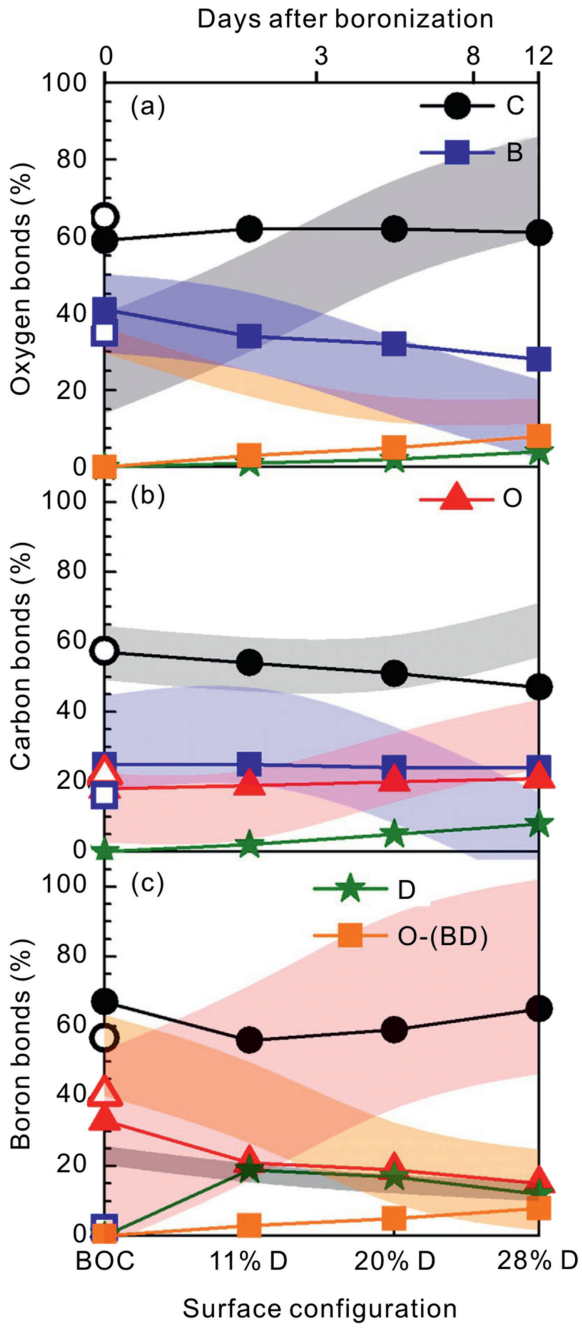

Fig. 11. Percentage of bonds of (a) O, (b) C, and (c) B to the other atoms in the BCOD surface in function of D concentration in the simulation cell. Small statistical errors, within the symbols size, were due to the random irradiation of the surface by 3000 D atoms at 5 eV impact energy, for each shown accumulated D concentration. The shaded colored areas, bands, are $\pm 1\sigma$ (σ is standard deviation) about the mean values measured by XPS of the corresponding bonding (color matched to the calculated values, gray is C, pink is O, light-blue is B, yellow is B-O-D), averaged over the 4 days of plasma exposure. The measured increase of the O-C bonding in (a) indicates increased dominance of oxygen atoms at the surface. *Figure reproduced from Ref.* [33] *with permission from the authors.*

though the simulations sometimes show coordination numbers of five and six, enabling more D atoms to bond to a B atom than to an oxygen atom (with typical coordination number of 2). Also electron withdrawing ligands on B such as O further

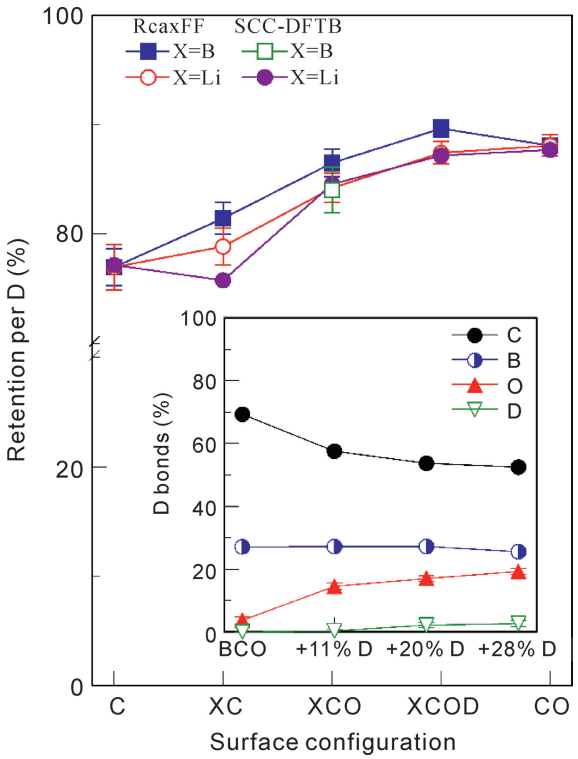

Fig. 12. Percentage of D bonds with constituents of the BCOD surface as function of the deuterium accumulated concentration (right axis) [33]. Boron is a main player in bonding and retaining D, unless D accumulation in the surface reach saturation when oxygen start playing important role in the D retention. Left axis: Retention per impact of D for various configurations of C, B, Li, O, D. Boron retains more, but not much more. QCMD-SCC-DFTB data are shown for the verification purposes.

increase D uptake on B. The role of B in the retention of D does not change with increasing D accumulation (Fig. 12).

4.2. Chemical sputtering

Chemical sputtering, unlike the retention probability, is strongly dependent on the impact energy. This energy dependence for the material matrices considered here is numerically highly intensive.

4.2.1. Chemical sputtering of lithiated carbon surface

The computational study of sputtering of lithiated and oxidized amorphous carbon surfaces by deuterium impact is performed in energy range 5–30 eV. Using REAXFF classical molecular dynamics the sputtering yields were obtained, the mass and energy spectra, as well as the angular distributions of ejected atoms and molecules of the surfaces saturated by accumulated deuterium impacts [63]. These results were successfully compared with the existing experimental and theoretical data for amorphous a-C:D surfaces. Presence of lithium reduces erosion of carbon, while presence of oxygen additionally reduces the erosion. The novel results in the paper are sputtering yields for various particles ejected from Li-C:D and Li-C-O:D surfaces. In absence of oxygen, the total carbon erosion is suppressed in comparison to a-C:D by about a factor of 2. However, Li contributes almost equally to carbon to the total sputtering at 30 eV, while its contribution at lower energies dominates sputtering due to the weak bond of Li to C. In presence of oxygen, the carbon erosion (40% in atomic form) is reduced by a factor of 4 in comparison to a-C:D, while Li sputtering (of which 75% is in atomic form) is reduced by a factor of 4 in comparison to Li-C:D (Fig. 14).

On the other hand, sputtering of hydrocarbon molecules (dominance of CD_3 and CD_4) of Li-C:D is increased by a factor of 2 in comparison to a-C:D, but reduced by a factor of 2 in presence of oxygen, as shown in Fig. 15. The presence of oxygen in lithiated carbon surface somewhat reduces C_2D_2 and the total ejection of hydrocarbons respect to the ATJ graphite [17,18]. The suppression of the ejected CD_3+CD_4 in these simulations is in good agreement with the analysis reported by P. Raman et al. [53] for a lithiated ATJ graphite and impacts of 1 keV D ions, and reported by Yagi et al. [55] for sputtering of ATJ graphite at 50–200 eV.

Fig. 16(a) presents the calculated sputtering yields for various lithium compounds ejected from the LiC:D and LiCO:D surfaces as functions of deuterium impact energy. These include the total sum of ejected atomic lithium and lithium compounds for each of the two surfaces. Sputtering yield of Li-D molecules decreases with energy for the LiC:D surface but seems to reach a maximum at 20 eV for the LiCO:D surface, being reduced by about a factor of 3 with presence of oxygen. When oxygen is present in the surface the dominant ejected product containing Li is Li-O molecule. Ejection of LiC molecules is not observed at energies below 30 eV due to the strong bond of the lithium and oxygen (~3.5 eV) inside the surface in comparison to more than a factor of 2 weaker Li-C bond (1.6 eV). Fig. 12(b) shows the calculated sputtering yields for various oxygen compounds ejected from the LiCO:D surface. Oxygen sputtering stays low, below 0.7%, over the whole studied energy range. Ejected molecules such as oxygen with deuterium (OD) and oxygen with carbon (CO) are the main products at the lowest impact energies, however, when the energy increases, a variety of oxygen compounds is present, such as OC, OLi, and OD.

4.2.2. Chemical sputtering of boronized carbon surface

A computational study of the chemical sputtering of boronized and oxidized amorphous carbon surfaces by deuterium irradiation is performed in range of impact energies 5–30 eV. As in case of lithiated surface the results were sputtering yields as well as mass, energy and angular spectra of ejected atoms and molecules of both virgin and deuterium saturated BCO surfaces. These were compared with the data for a deuterated BC surface and existing theoretical and experimental results for amorphous C:D. Boron significantly (stronger than lithium) suppresses the erosion of carbon. This effect is further enhanced by presence of oxygen, with total carbon yields per D, mainly CD_3 and CD_2, staying in the range below 0.2%. While in case of the lithiated surfaces CD and LiD are dominating the sputtered material, potentially emitted into the plasma, CD and D_2O are dominating the emitted molecules from boronized surfaces, which becomes exclusively D_2O with increase of the D accumulation. OD and O are the dominant

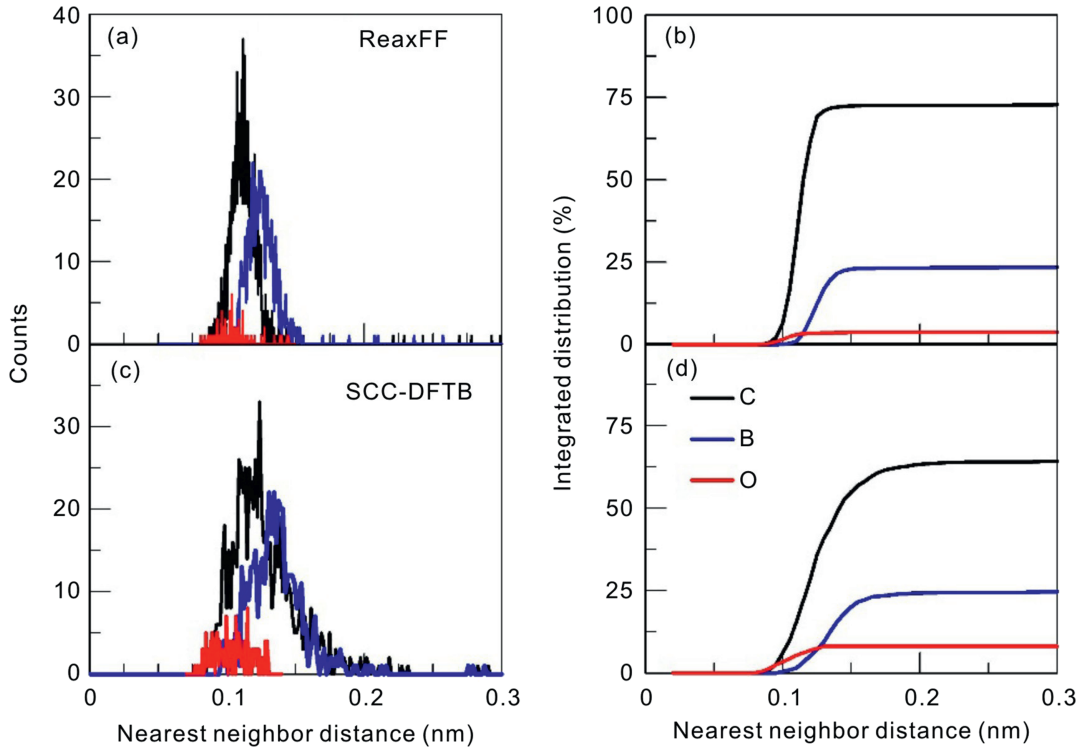

Fig. 13. Nearest neighbor analysis for retained D trajectories in a sample of 20% of boron and oxygen in the carbon, prepared by ReaxFF in LAMMPS in (a) and (b) and by QCMD with SCC-DFTB in (c) and (d). Both approaches show the effect of the oxygen suppression in the retention chemistry, though with slightly different cumulative numbers and the distribution widths.

sputtered particles from BCO:D surface (Fig. 17), with yields ranging from 0.5% to almost 2%. Sputtering yield of D_2O reaches 1% at lower energies, to be replaced with atomic oxygen at higher energies. Translational energy for ejected oxygen atoms and OD_x molecules of BCO:D surface are in the range 1−2 eV, which is higher than energy of sputtered CD_x molecules (around 1 eV).

Fig. 18 shows the mass spectra of various CD_x molecules characterized by their mass, ejected from the BCO:D surface over the studied impact energy range 5−30 eV of D. CD_3 followed by CD_2 and CD are the leading sputtered product at 20 eV and 30 eV, while at 10 eV it is CD_2 followed by CD_3 and CD. At 5 eV, CD and CD_2 is followed by CD_3. We note that the suppression of carbon erosion is significantly enhanced with the presence of oxygen in the boronized carbon surface. Thus, the sputtered CD_3 is reduced about 3 times and CD_2 about five times for the BCO:D surface in comparison to the BC:D surface at 30 eV (not shown in Fig. 18). In Fig. 18(b), we present the sputtered OD_x molecules and oxygen atoms for various impact energies. The leading product at 20 eV and 30 eV is atomic oxygen, while water (OD_2 molecules) is dominant at energies 5 eV and 10 eV.

4.2.3. Temperature effects in BCO:D surface[1]

The preparation of an amorphous boronized and oxidated carbon surface (BCO) is crucial and the first step in the theoretical treatment of the BCO:D surface to change of temperature in range 300−1000 K. A BCO surface is defined as a computer cell of 400 atoms with an initial atomic distribution of 20% of both O and B, and 60% of C. These percentages are reflecting the experimental data in the NSTX-U [56]. The surface cell has dimensions of 1.75 nm × 1.75 nm × 2.0 nm to prevent reflections from the bottom of the cell by the impinging D atoms. Periodic boundary conditions in *x* and *y* directions are applied to simulate an infinite surface. The target is energy optimized by heating and annealing processes, followed by a thermalization process to a required target temperature by using a Langevin thermostat with a time constant of 100 fs [78].

The BCO surface is deuterated by a cumulative D bombarding process at each impact energy (10 and 15 eV) and target temperature (300−1000 K). The process starts by shooting one deuterium atom on an amorphous BCO surface, the projectile velocity is orthogonal to the cell surface in the *z*-direction and this process lasts 20 ps. The target is then thermalized at the chosen temperature for another 20 ps, followed by a relaxation process of the whole system for 10 ps. This procedure is repeated until the surfaces reaches a deuterium saturation state, the BCO:D surface [41,63,64]. Calculation of the amount of deuterium accumulated in the surface, D_{acc}, follows the equation

$$D_{acc} = \frac{N_D}{N_C + N_B + N_O + N_D}, \quad (1)$$

where N_D is the number of deuterium atoms accumulated at each impact; N_C, N_B, and N_O are instantaneous number of carbon, boron, and oxygen atoms, respectively. In Fig. 19 we

[1] This material has not been published previously.

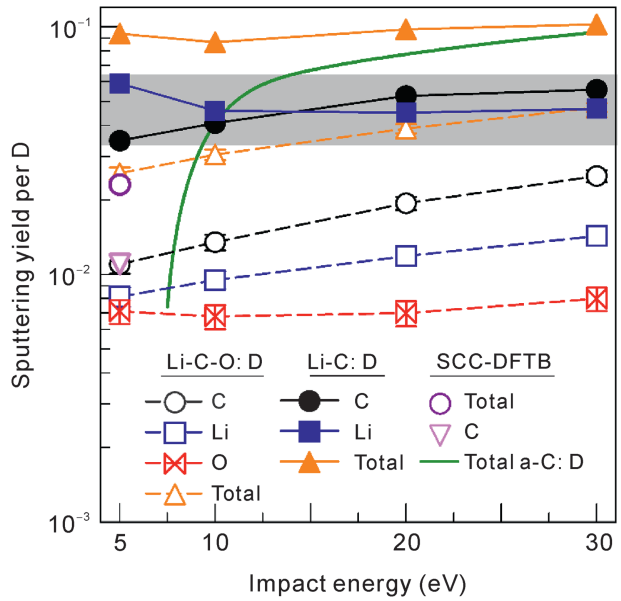

Fig. 14. Total sputtering yields (including molecules) for C and Li of LiC:D, and for C, Li, and O from the LiCO:D surface [63]. Presence of oxygen in the LiC mixture reduces the sputtering of carbon and lithium. The results are compared with total sputtering yield of a-C:D surface [40] as well as with the normalized data obtained by SCC-DFTB at 5 eV impact energy [6]. Gray band in the upper part represents the experimental result of lithium sputtering yield [32,77].

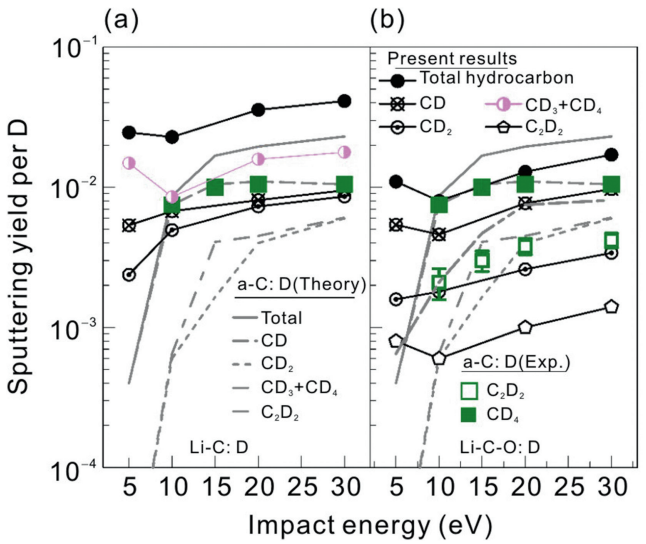

Fig. 15. The total, CD, CD_2, and CD_3+CD_4 sputtering yields per D as function of the impact energy for (a) LiC:D surface and for (b) LiCO:D surface. The calculated results are compared with the theoretical [44] and experimental data [70,71] for a-C:D. Ejection of CD_4 molecules is not observed for the LiCO:D (Fig. 12(b) is in good agreement with the results of Yagi et al. [55]. *Figure reproduced from Ref.* [63] *with permission from the authors.*

show the percentage of deuterium accumulated in the surface as function of the number of D impacts, for different target temperatures. The saturation state of the surface is reached when the variation of D_{acc} is less than 0.5%. The maximum value of D saturation is ~28% at target temperatures of 300 and 400 K, then this value decreases for higher temperatures of the surface.

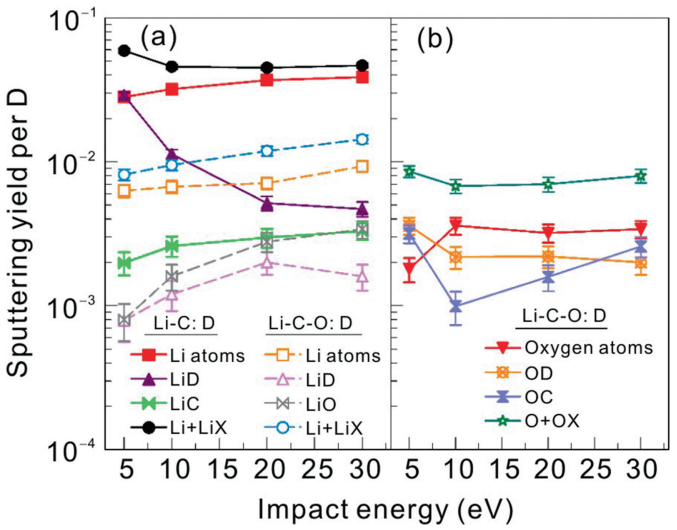

Fig. 16. (a) Sputtering yield per D for ejected lithium atoms and Li-X molecules, from the LiC:D and LiCO:D surfaces as function of the impact energy. X = D, C, or O; Li + LiX means total yield of lithium atoms and all lithium compounds ejected. (b) O + OX is the total yield of oxygen atoms and all ejected combinations for oxygen molecules. *Figure reproduced from Ref.* [63] *with permission from the authors.*

Also, the maximum percentage of D saturation for an amorphous carbon surface is $(n_H/n_C) \times 100\% \approx 40\%$ (n_H is the number of H atoms and n_C is the number of C atoms) [79], and it can be written as $[n_H/(n_C + n_H)] \times 100\% = 28.57\%$. This value is close to the maximum for a BCO surface.

The obtained BCO:D surface is bombarded by 15,000 D impacts at 10 and 15 eV for each target temperature. The calculation was done by LAMMPS, using REAXFF potentials and EEM. The impinging deuterium atoms are initially uniformly distributed at a distance of 0.7 nm above the surface, and their velocities are parallel to the surface normal. The MD simulations are performed for 50 ps, in a successive series of independent 15,000 trajectories. Fig. 20 shows the total ejection yield of ejected carbon atoms per D as function of the surface temperature. The calculated results are shown at impact energies of 10 eV in Fig. 20(a) and 15 eV in Fig. 20(b). The results of the CMD simulations are compared with theoretical and experimental results for an a-C:D surface [50,52]. The carbon erosion is suppressed by the presence of boron in the carbon surface. It decreases by a factor of four at 10 eV and a factor of two in average at 15 eV, with respect to the experimental results for a-C:D surface by Mech et al. [46]. The results follow qualitatively the trend presented by the experimental data of Mech *et al.* [46] at 15 eV impact energy. However, the carbon erosion is suppressed by a factor of 10 according to the experimental data of Balden et al. [49]. For both impact energies, the calculated total ejection yield reaches its maximum at 500 K and then decreases for higher surface temperatures.

Fig. 21 presents the sputtering yield per D for ejected CD*x* molecules and C atoms, as function of the target temperature. The results in Fig. 21(a) are for 10 eV impact energy. The main ejected product is atomic carbon at the lowest temperature, while complexity of molecules (CD and CD_2) increases

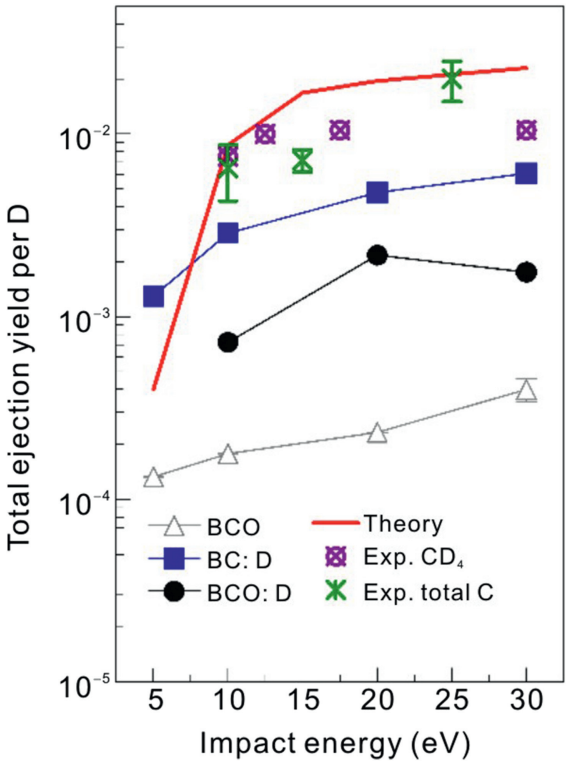

Fig. 17. Total ejection yield per D of carbon from virgin BCO (empty triangle), BC:D (solid square), and BCO:D (solid circle) surfaces as function of the impact energy. These results are compared with reported simulation data for a-C:D as well as with experimental data for CD_3+CD_4 (cross points) sputtering yield and with total C ejected (asterisk points) from polycrystalline graphite. *Figure reproduced from Ref.* [64] *with permission from the authors.*

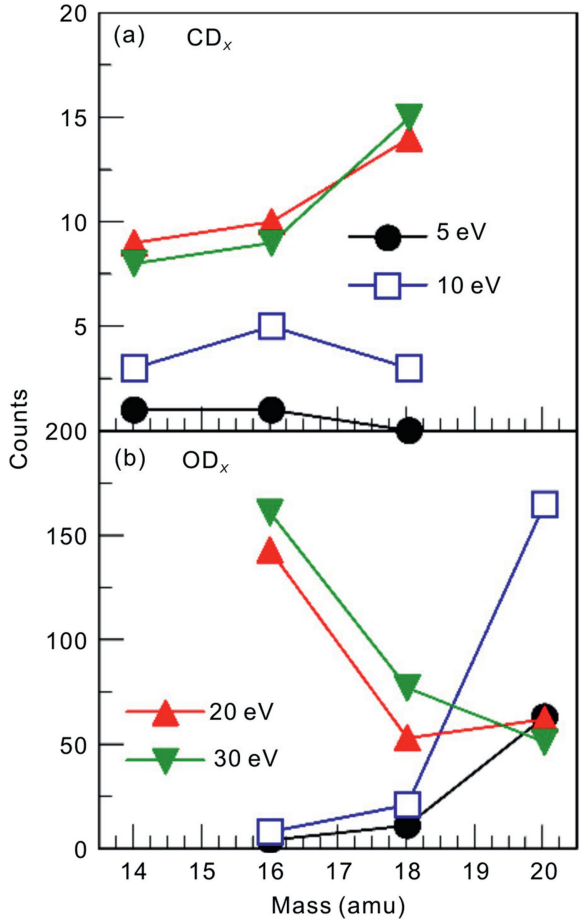

Fig. 18. Mass spectra of (a) CD_x molecules and (b) OD_x molecules and oxygen atoms ejected from the BCO:D surface as function of impact energy of D [63].

with the surface temperature. The CD and CD_2 molecules are dominant at the temperatures higher than 600 K. However, the ejection of CD_3 and CD_4 molecules is the lowest in the whole temperature range. In Fig. 21(b) ejection of CD dominates all considered surface temperatures. Ejection of CD_4 molecules is reduced by a factor of 10 with respect to the a-C:D ejection [46] of CD_4 in the whole temperature range. Even though the impact energy is 15 eV, the ejection yield of CD_3+CD_4 molecules is the lowest with respect to other carbon species at the whole temperature range.

Fig. 22 shows ejection yield of sputtered oxygen atoms, OD*x* and CO molecules as function of the targeted temperature. D_2O molecules have the biggest contribution to the total ejection per D in the whole considered temperature range and for both impact energies. Ejection of oxygen atoms and its species increases as function of the surface temperature. The ejection of CO molecules increases as function of the surface temperature at 10 eV (Fig. 22(a)), but it decreases for surface temperatures higher than 600 K at 15 eV (Fig. 22(b)).

5. Role of oxygen in low-*Z* mixtures with metallic substrates

With the established understanding of the role that oxygen together with lithium and boron play on hydrogen retention in graphitic substrates, the next question is how does this behavior extrapolate to other candidate fusion PFC materials exposed to extreme conditions? Other candidate materials include beryllium and tungsten. Beryllium, due to its electropositive nature compared to oxygen and carbon, for example, would behave somewhere between lithium and boron given its electronegativity value is 1.57 compared to

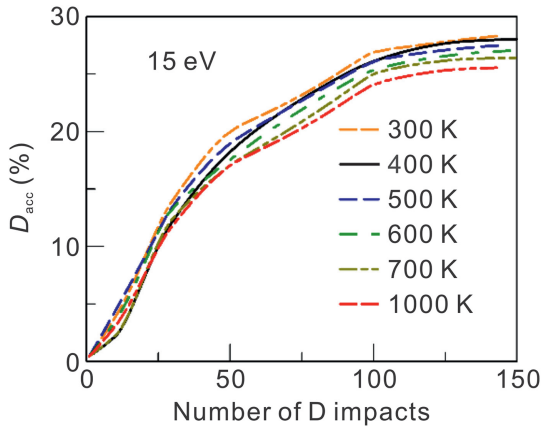

Fig. 19. Percentage of deuterium accumulated D_{acc} in the amorphous boronized and oxidated carbon surface as function the D impacts, at 15 eV impact energy, for various temperatures.

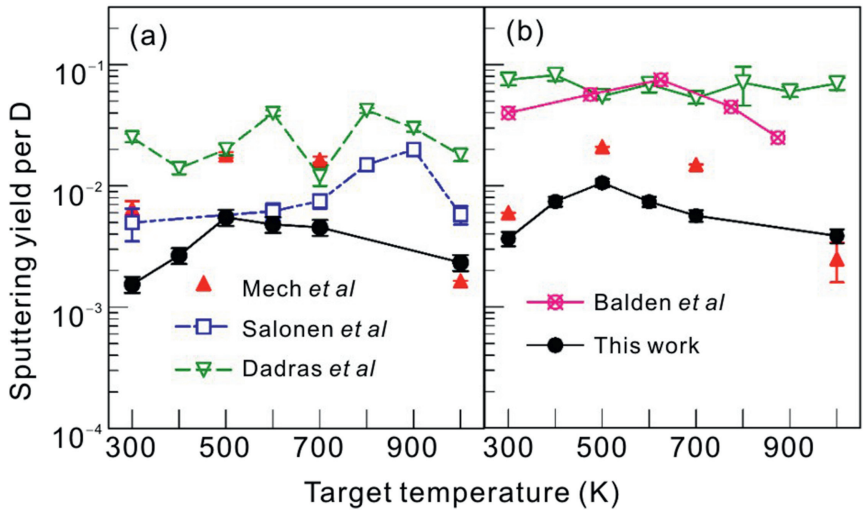

Fig. 20. Total ejection yield per D of ejected carbon atoms and its compounds (CDx), as function of the target temperature. The results for impact energies of 10 eV in (a), and 15 eV in (b) are compared with the theoretical results for a-C:D surface by computations of Salonen et al. [50] and Dadras et al. [52], as well as with experimental data of Mech et al. [46] and Balden et al. [49].

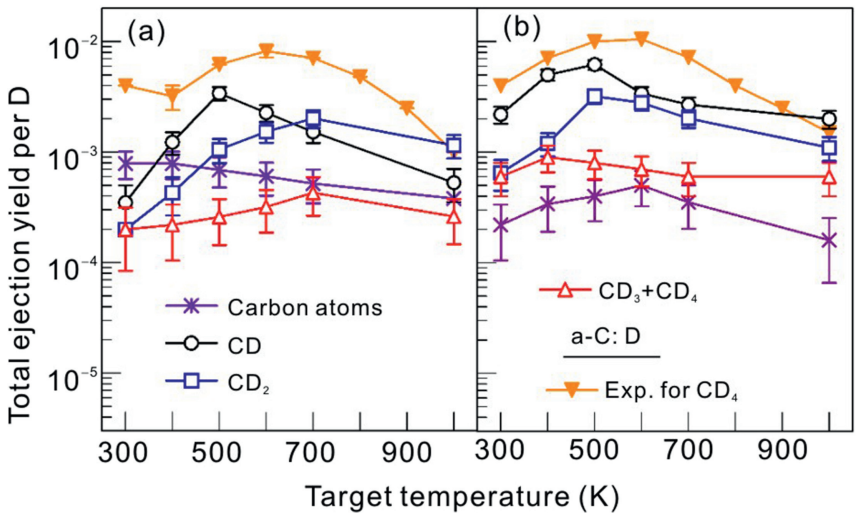

Fig. 21. Ejection yield of sputtered CDx molecules and C atoms as function of the target temperature, for impact energies of 10 eV in (a) and 15 eV in (b), compared with experimental results for a-C:D surface [46], showing the suppresion of carbon erosion by the presence of boron in the carbon surface.

0.98 and 2.04 for Li and B, respectively. The case of tungsten or other high-Z materials can be more complicated given the propensity of electron emission and oxide formation. In addition, the complexity of irradiation-driven mechanisms that were identified as important drivers of oxygen and deuterium retention are coupled to the complex irradiation response of tungsten, which have significantly different radiation damage properties compared to graphitic substrates. Studies have examined the combination of low-Z coatings on high-Z substrates as an application to fusion PFCs. In this context we can examine any similarities to behavior identified earlier in this review on the role oxygen plays on hydrogen retention of lithium thin-films on high-Z substrates (e.g. W or Mo).

The first *in-situ* studies of lithium thin-film coatings on refractory metal (high-Z) substrates was conducted by Heim et al. and demonstrated a tendency for enhanced hydrogen retention with the presence of oxides during deuterium irradiation [80]. Fig. 23 shows the O1s XPS spectra similar to studies conducted for lithiated graphite where the peaks for metallic oxides are differentiated from the chemical complex associated to Li-O-D bonding at a binding energy between 532 and 534 eV. During D irradiation it was found that a similar chemical complex is found where the role of lithium and oxygen is critical for the retention of hydrogen on metallic substrates. The result is intriguing in that the collisional effects are quite different between metallic and graphitic substrates yet the effects on hydrogen isotope retention have important similarities. First, the physical mechanism is distinctly different between bombarding a lithium thin-film coating on a graphite compared to a molybdenum substrate with deuterium energetic particles. The implanted deuterium atoms immediately bind chemically to the graphite substrate, while the low

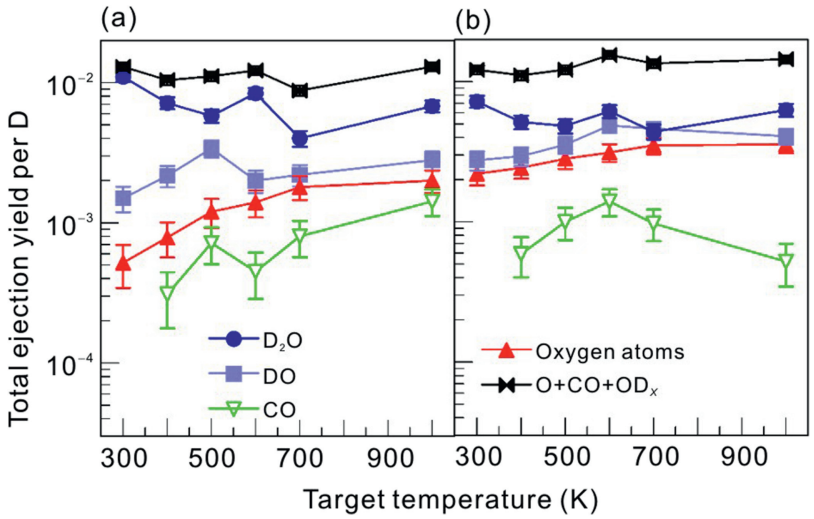

Fig. 22. Ejection yield per D for sputtered oxygen atoms and OD*x* molecules, as function of the target temperature. The considered impact energy is 10 eV in (a) and 15 eV in (b).

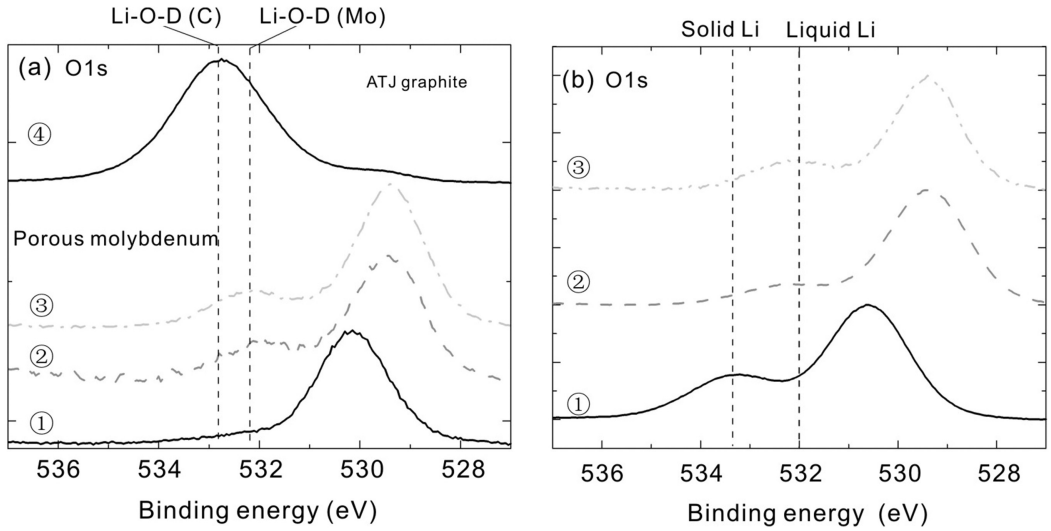

Fig. 23. (a) O1s XPS spectra of porous Mo for various sample conditions: ① porous molybdenum after 3 μm of lithium deposition, ② with 3 μm of lithium deposition and exposure to $3.6 \times 10^{15} D_2^+$ cm^{-2} fluence at 250 °C, ③ with 3 μm of lithium deposition and exposure to $1.0 \times 10^{17} D_2^+$ cm^{-2} fluence at 250 °C, ④ ATJ graphite after 2 μm Li deposition and $1.0 \times 10^{17} D_2^+$ cm^{-2} fluence at room temperature. (b) O1s XPS spectra for similar Mo substrate: ① 3 μm of lithium deposition and 1.5×10^{16} D_2^+ cm^{-2} at room temperature, ② 2 μm of lithium deposition at room temperature and 1.5×10^{16} D_2^+ cm^{-2} at 250 °C, and ③ 3 μm lithium deposition at 250 °C and 1.5×10^{16} D_2^+ cm^{-2} at the same temperature [80].

energy transfer factor of D-Mo results in a large backscattering yield of D atoms from the underlying Mo substrate back to the lithium thin-film region enhancing the concentration of D atoms near the surface. The lithium affinity for oxygen chemically attracts the deuterium atoms thus increasing the probability for Li-O-D formation near the surface. As the temperature is increased the probability for diffusivity of both Li and D is increased and thus diffusion of D into the bulk is more likely, which decreases the amount of Li-O-D observed by XPS, which only probes down to about 5 nm of the surface. This is consistent with the observed behavior in the *in-situ* XPS experiments and confirms the mechanisms predicted by the computational simulations used to study lithium-oxide hydrogen interactions by Krstic et al. [6]. The key findings on metallic substrates were corroborated by further studies by Neff et al. [81], where Li thin-films were deposited on a variety of tungsten substrate allotropes (i.e. porous W, refined-grained W, nanocrystalline W, W alloys) also demonstrating a tendency for hydrogen isotope retention by oxide-lithium presence at the surface.

Neff et al. [81] discovered a similar tendency as found by Heim et al. for lithium thin-films retaining hydrogen isotopes when oxygen is present. Fig. 24 shows the O1s spectra for a number of irradiation *in-situ* exposures of Li thin-films on tungsten substrates. These experiments examined not only the effect of Li thin-films to retain deuterium under extreme irradiation conditions but also identified a new mechanism whereby if the particle beam was mixed with an inert particle

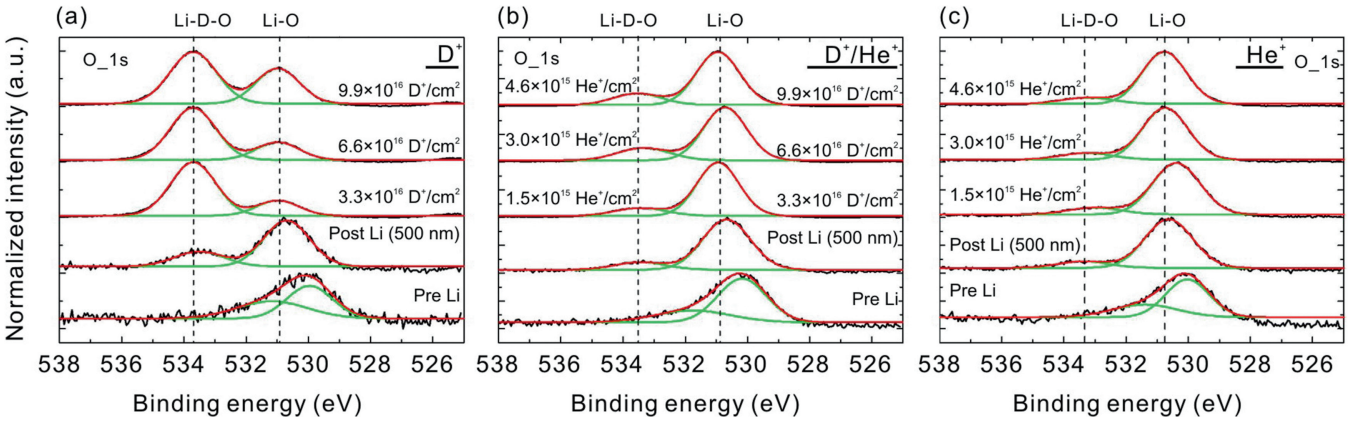

Fig. 24. O1s XPS spectra of 500 nm lithium thin-films on polished commercial-grade W substrates at room temperature from "pre-Li" conditions (bottom spectra) on W surface to "post-Li" conditions (second to bottom spectra) to irradiated conditions: (a) from 3.3×10^{16} $D_2^+cm^{-2}$ fluence to ~1.0×10^{17} $D_2^+cm^{-2}$ fluence, (b) same D^+ fluences with 10% He mixed energetic particle beam with He^+ fluences between 1.5×10^{15} He^+cm^{-2} to 4.6×10^{15} He^+cm^{-2}, and (c) using only He^+ irradiation (e.g. control) with fluences from 1.5×10^{15} He^+cm^{-2} to 4.6×10^{15} He^+cm^{-2} [76].

source (i.e. helium particles), the amount of deuterium retained could be controlled.

Indeed, the experiments confirmed this conjecture as shown in Fig. 24(b) where the mixed beam with about 10% He demonstrated that the Li-O-D functionality would not grow even with the increasing deuterium fluence as in the "D-only" case in Fig. 24(a). The control case where only an inert particle source was used (e.g. the case using He only) also demonstrated (as in many other experiments, e.g. [74] and [41], that the Li-O-D functionality is strictly due to the exposure to energetic D particles and the presence of both lithium and oxygen, a mechanism predicted by the computational simulation work of Krstic et al. This is further corroborated in the recent results by Neff et al.[2] [81] on *in operando* irradiation data whereby XPS of the Li-O-D functionality and Li-O chemical bond is measured during irradiation exposure to He sequenced by D energetic particles. In this experiment, Fig. 25(a) shows the results for the case of He-only irradiation, where there is no sign of Li-O-D complex. This step is then followed by first shutting off the He beam and then exposing the surface to the D+ ions consequently leading to the observed Li-O-D complex that grows with D fluence. Finally, this low-fluence D exposure is followed by He irradiation which results in the inert energetic He particles breaking up the Li-O-D bonding and consequently decreasing the D retention (e.g. lowering the Li-O-D/Li_2O area ratio). However, there seems to be a saturation point after which after larger D^+ fluences of the order of 10^{16} cm^{-2} as shown in Fig. 25(b), implanted energetic He can drive oxygen from sub-surface regions to the surface *maintaining* deuterium retention there. These *in operando* results confirmed for the first time that a controlled amount of He in a D particle beam flux can control the amount of D retention on a lithiated surface on metallic substrates such as tungsten.

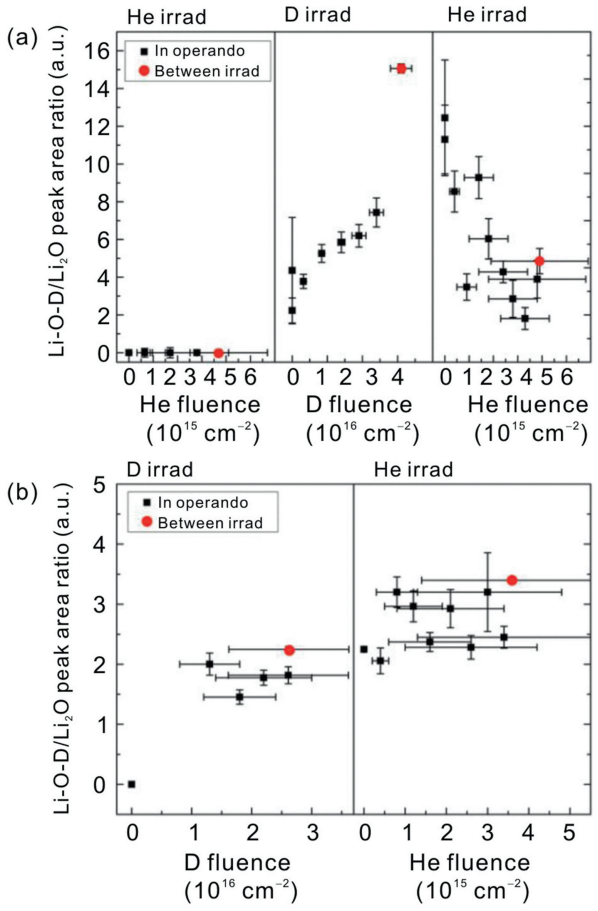

Fig. 25. (a) *In operando* Li-O-D/Li_2O peak area ratio derived from O1s XPS spectra of Li/W system exposed to He irradiation sequenced by D irradiation and He irradiation showing the effect of ballistic bond-breaking mechanism of He of the Li-O-D surface complex. (b) D irradiation followed by simultaneous He irradiation with water vapor exposure showing enhanced LiOH from oxygen reduction during irradiation.

6. Conclusions

The coupling between fusion material surfaces and the plasmas that interact with them has challenged our

[2] Experimental results reported in doctoral thesis of Neff [81], previously not published.

understanding of these extreme environments. The interaction of energetic particles drives materials far from equilibrium, resulting in dynamic changes to surface chemistry and physics at the plasma-material interface. Recent work coupling both *in-situ* and *in operando* experimental measurements with advanced multi-scale computational tools have ushered a new understanding of irradiation surface science unraveling the chemistry and physics of these complex interfaces. In particular, this review summarizes the role of lithium coatings applied on a variety of graphitic and metallic surfaces in a number of tokamak fusion machines and benchtop *in-situ* experiments. Conditioning fusion device wall materials with lithium have demonstrated a subtle interplay of the lithiated plasma facing surfaces and plasma properties. In one example, the Li presence in the NSTX (National Spherical Tokamak Experiment) plasma extreme environment led to a lower H-mode power threshold, increased plasma power, increased discharge times and reduced fuel recycling. Studies of lithiated carbon surfaces also identified a peculiar physical effect of the intercalated lithium presence when exposed to deuterium irradiation: a dramatic increase of the oxygen concentration in the top layers of the surface. The increased oxygen concentration is responsible for the chemistry of deuterium retention and sputtering, while lithium mainly plays the role of a catalyzer in this process. This understanding completely transformed the community understanding on the deuterium retention mechanism in the lithium-based surfaces as shown by both quantum-classical molecular dynamics computations and by laboratory experiments. In case of carbon boronization, boron plays together with oxygen an active role in D retention and causes significant suppression of the chemical sputtering at impact energies of deuterium below 30 eV. The computed chemistry in the BCOD surface was validated by the first *in situ-ex tempore* experiments using the MAPP (Material Analysis Particle Probe) diagnostic platform inside the NSTX fusion chamber. The computational study of the effects of the sputtering suppression in boronized carbon surfaces shows that the suppression of sputtering extends to surface temperatures as high as 1000 K. Studies with lithium thin-films on metallic substrates such as W and Mo also demonstrate a tendency for enhanced D retention via Li-O-D interactions and irradiation-driven effects influencing the amount of D retained.

Conflict of interest

We do not have any conflict of interest.

Acknowledgements

Research supported by the USDOE OFES grant DE-SC0013752 through RF of SUNY (PSK), by USDOE BES/FES Grant No. DE-SC0010717 (JPA and FB) and by the National Council for Science and Technology of Mexico (CONACyT) through the postdoctoral fellowship # 267898 (FJDG). The authors would like to thank Stony Brook Research Computing and Cyber Infrastructure of the Institute for Advanced Computational Science at Stony Brook University; To Extreme Science and Engineering Discovery Environment (XSEDE), which is supported by National Science Foundation grant number ACI-1548562.XSEDE (UCSD's Comet and TACC's Stampede) as well as to Director's Discretion Program of ORNL for access to the supercomputing facilities of OLCF (Titan and Eos).

References

[1] A.W. Leonard, M.A. Mahdavi, S.L. Allen, N.H. Brooks, M.E. Fenstermacher, et al., Distributed divertor radiation through convection in DIII-D, Phys. Rev. Lett. 78 (1997) 4769.
[2] C. Abromeit, Aspects of simulation of neutron damage by ion irradiation, J. Nucl. Mat. 216 (1994) 78.
[3] A. Kallenbach, J. Adamek, L. Aho-Mantila, S. Äkäslompolo, C. Angioni, et al., Overview of ASDEX upgrade results, Nucl. Fusion 51 (2011) 094012.
[4] V.A. Soukhanovskii, R. Maingi, D.A. Gates, J.E. Menard, S.F. Paul, et al., Divertor heat flux mitigation in high-performance H-mode discharges in the National Spherical Torus Experiment, Nucl. Fusion 49 (2009) 095025.
[5] G. Federici, C.H. Skinner, J.N. Brooks, J.P. Coad, C. Grisolia, et al., Plasma-material interactions in current tokamaks and their implications for next step fusion reactors, Nucl. Fusion 41 (2001) 1967.
[6] P.S. Krstic, J.P. Allain, C.N. Taylor, J. Dadras, S. Maeda, et al., Deuterium uptake in magnetic-fusion devices with lithium-conditioned carbon walls, Phys. Rev. Lett. 110 (2013) 105001.
[7] C.N. Taylor, B. Heim, J.P. Allain, Chemical response of lithiated graphite with deuterium irradiation, J. Appl. Phys. 109 (2011) 053306.
[8] S.J. Zinkle, Fusion materials science: overview of challenges and recent progress, Phys. Plasmas 12 (2005) 058101.
[9] C.H. Skinner, R. Sullenberger, B.E. Koel, M.A. Jaworski, H.W. Kugel, Plasma facing surface composition during NSTX Li experiments, J. Nucl. Mat. 438 (2013) S647.
[10] C.H. Skinner, J.P. Allain, W. Blanchard, H.W. Kugel, R. Maingi, et al., Deuterium retention in NSTX with lithium conditioning, J. Nucl. Mater. 415 (2011) S773.
[11] F. Ghezzi, L. Laguardia, R. Caniello, A. Canton, S. Dal Bello, et al., XPS, SIMS and FTIR-ATR characterization of boronized graphite from the thermonuclear plasma device RFX-mod, Appl. Surf. Sci. 354 (2015) 408.
[12] G. Federici, P. Andrew, P. Barabaschi, J. Brooks, R. Doerner, et al., Key ITER plasma edge and plasma−material interaction issues, J. Nucl. Mater. 313 (2003) 11−22.
[13] J. Winter, Wall conditioning in fusion devices and its influence on plasma performance, Plasma Phys. Control. Fusion 38 (1996) 1503.
[14] R. Maingi, S.M. Kaye, C.H. Skinner, D.P. Boyle, J.M. Canik, et al., Continuous improvement of H-mode discharge performance with progressively increasing lithium coatings in the National Spherical Torus Experiment, Phys. Rev. Lett. 107 (2011) 145004.
[15] F. Bedoya, J.P. Allain, R. Kaita, C.H. Skinner, B.E. Koel, et al., Initial studies of plasma facing component surface conditioning in the national spherical tokamak experiment upgrade with the materials analysis particle probe, Nucl. Mater. Energy 12 (2017) 1248−1252.
[16] C.H. Skinner, F. Bedoya, F. Scotti, J.P. Allain, W. Blanchard, et al., Advances in boronization on NSTX-Upgrade, Nucl. Mater. Energy 12 (2017) 744−748.
[17] C.N. Taylor, Fundamental Mechanisms of Deuterium Retention in Lithiated Graphite Plasma Facing Surfaces, Doctoral thesis, Purdue University, West Lafayette, IN, USA, 2012.
[18] F. Bedoya, J.P. Allain, R. Kaita, C.H. Skinner, L. Buzi, et al., Unraveling wall conditioning effects on plasma facing components in NSTX-U with the Materials Analysis Particle Probe (MAPP), Rev. Sci. Instrum. 87 (2016) 11D403.
[19] C.N. Taylor, J.P. Allain, B. Heim, P.S. Krstic, C.H. Skinner, et al., Surface chemistry and physics of deuterium retention in lithiated graphite, J. Nucl. Mat. 415 (2011) S777.

[20] C.N. Taylor, J. Dadras, K.E. Luitjohan, J.P. Allain, P.S. Krstic, et al., The role of oxygen in the uptake of deuterium in lithiated graphite, J. Appl. Phys. 114 (2013) 223301.
[21] C. Hollenstein, B.P. Duval, T.D. de Wit, B. Joye, H.J. Künzli, et al., Cold boronisation in TCA, J. Nucl. Mater. 176 (1990) 343.
[22] O.I. Buzhinskij, Y.M. Semenets, Review of in situ boronization in contemporary tokamaks, Fusion Sci. Technol. 32 (1997) 1−13.
[23] M. Lucia, R. Kaita, R. Majeski, F. Bedoya, J.P. Allain, et al., Dependence of LTX plasma performance on surface conditions as determined by in situ analysis of plasma facing components, J. Nucl. Mater. 463 (2015) 907.
[24] H. Kugel, D. Mansfield, R. Maingi, M.G. Bell, R.E. Bell, et al., Evaporated lithium surface coatings in NSTX, J. Nucl. Mater. 390 (2009) 1000.
[25] H.W. Kugel, M.G. Bell, J.W. Ahn, J.P. Allain, R. Bell, et al., The effect of lithium surface coatings on plasma performance in the National Spherical Torus Experiment, Phys. Plasma 15 (2008) 056118.
[26] R. Maingi, R. Kaita, F. Scotti, V.A. Soukhanovskii, The NSTX team, Elimination of inter-discharge helium glow discharge cleaning with lithium evaporation in NSTX, Nucl. Mater. Energy 12 (2017) 720.
[27] D.L. Rudakov, C.P.C. Wong, A. Litnovsky, W.R. Wampler, J.A. Boedo, et al., Overview of the recent DiMES and MiMES experiments in DIII-D, Phys. Scr. T138 (2009) 14007.
[28] J.P. Allain, A. Shetty, Unraveling atomic-level self-organization at the plasma-material interface, J. Phys. D 50 (2017) 283002.
[29] M. Rubel, S. Brezinsek, J.W. Coenen, A. Huber, A. Kirschner, et al., Overview of wall probes for erosion and deposition studies in the TEXTOR tokamak, Matter Radiat. Extremes 2 (2017) 87.
[30] G.M. Wright, H.A. Barnard, L.A. Kesler, E.E. Peterson, P.W. Stahle, et al., An experiment on the dynamics of ion implantation and sputtering of surfaces, Rev. Sci. Instrum. 85 (2014) 23503.
[31] G.M. Wright, D.G. Whyte, B. Lipschultz, R.P. Doerner, J.G. Kulpin, Dynamics of hydrogenic retention in molybdenum: first results from DIONISOS, J. Nucl. Mater. 363 (2007) 977−983.
[32] S.M. Kaye, T. Abrams, J.-W. Ahn, J.P. Allain, R. Andre, et al., An overview of recent physics results from NSTX, Nucl. Fusion 55 (2015) 104002.
[33] F.J. Domínguez-Gutiérrez, F. Bedoya, P.S. Krstić, J.P. Allain, S. Irle, et al., Unraveling the plasma-material interface with real time diagnosis of dynamic boron conditioning in extreme tokamak plasmas, Nucl. Fusion 57 (2017) 086050.
[34] L. Pauling, The nature of the chemical bond. IV. The energy of single bonds and the relative electronegativity of atoms, J. Am. Chem. Soc. 54 (1932) 3570.
[35] S. Brezinsek, A. Widdowson, M. Mayer, V. Philipps, P. Baron-Wiechec, et al., Beryllium migration in JET ITER-like wall plasmas, Nucl. Fusion 55 (2015) 063021.
[36] K. Heinola, J. Likonen, T. Ahlgren, S. Brezinsek, G. De Temmerman, et al., Long-term fuel retention and release in JET ITER-like wall at ITER-relevant baking temperatures, Nucl. Fusion 57 (2017) 086024.
[37] W.J. Mortier, S.K. Ghosh, S. Shankar, Electronegativity-equalization method for the calculation of atomic charges in molecules, J. Am. Chem. Soc. 108 (1986) 4315.
[38] Y. Cong, Z.-Z. Yang, General atom-bond electronegativity equalization method and its application in prediction of charge distributions in polypeptide, Chem. Phys. Lett. 316 (2000) 324.
[39] P.S. Krstic, R.J. Harrison, B. Sumpter, Excited state quantum-classical molecular dynamics, Phys. Scr. T124 (2006) 101.
[40] P.S. Krstic, C.O. Reinhold, S.J. Stuart, Energy and angle spectra of sputtered particles for low-energy deuterium impact of deuterated amorphous carbon, J. Appl. Phys. 104 (2008) 103308.
[41] F.J. Domínguez-Gutiérrez, F. Bedoya, P.S. Krstić, J.P. Allain, A.L. Neff, et al., Studies of lithiumization and boronization of ATJ graphite PFCs in NSTX-U, Nucl. Mater. Energy 12 (2017) 334.
[42] A.Y.K. Chen, J.W. Davis, A.A. Haasz, Methane formation in graphite and boron-doped graphite under simultaneous O^+ and H^+ irradiation, J. Nucl. Mat. 290 (2001) 61.
[43] J. Kuppers, The hydrogen surface chemistry of carbon as a plasma facing material, Surf. Sci. Rep. 22 (1995) 249.
[44] P.S. Krstic, C.O. Reinhold, S.J. Stuart, Chemical sputtering from amorphous carbon under bombardment by deuterium atoms and molecules, New J. Phys. 9 (2007) 209.
[45] H. Zang, F.W. Mayer, H.M. Meyer III, M.J. Lance, Surface modification and chemical sputtering of graphite induced by low-energy atomic and molecular deuterium ions, Vacuum 82 (2008) 1285.
[46] B.V. Mech, A.A. Haasz, J.W. Davis, Isotopic effects in hydrocarbon formation due to low-energy H^+/D^+ impact on graphite, J. Nucl. Mater. 255 (1998) 153.
[47] P. Norajitra, S.I. Abdel-Khalik, L.M. Giancarli, T. Ihli, G. Janeschitz, et al., Divertor conceptual designs for a fusion power plant, Fusion Eng. Des. 83 (2008) 893.
[48] R.A. Pitts, S. Carpentier, F. Escourbiac, T. Hirai, V. Komarov, et al., Physics basis and design of the ITER plasma-facing components, J. Nucl. Mater. 415 (2011) S957.
[49] M. Balden, J. Roth, New weight-loss measurements of the chemical erosion yields of carbon materials under hydrogen ion bombardment, J. Nucl. Mater. 280 (2000) 39.
[50] E. Salonen, K. Nordlund, J. Keinonen, C.H. Wu, Swift chemical sputtering of amorphous hydrogenated carbon, Phys. Rev. B 63 (2001) 195415.
[51] E.D. de Rooij, U. von Toussaint, A.W. Kleyn, W.J. Goedheer, Molecular dynamics simulations of amorphous hydrogenated carbon under high hydrogen fluxes, Phys. Chem. Chem. Phys. 11 (2009) 9823.
[52] J. Dadras, P.S. Krstic, Chemical sputtering of deuterated carbon surfaces at various surface temperatures, Nucl. Instr. Meth. Phys. Res. B 269 (2011) 1280.
[53] P. Raman, A. Groll, P. Fiflis, D. Curreli, D. Andruczyk, et al., Chemical sputtering studies of lithiated ATJ graphite, J. Nucl. Mater. 438 (2013) S655.
[54] M. Racic, K. Ibano, R. Raju, D.N. Ruzic, Physical erosion studies of plain and lithiated graphite, J. Nucl. Mater. 390 (2009) 1043.
[55] H. Yagi, H. Toyoda, H. Sugai, Dramatic reduction of chemical sputtering of graphite under intercalation of lithium, J. Nucl. Mater. 313 (2003) 284.
[56] P.S. Krstic, J.P. Allain, A. Allouche, J. Jakowskie, J. Dadras, et al., Dynamics of deuterium retention and sputtering of Li−C−O surfaces, Fusion Eng. Des. 87 (2012) 1732.
[57] M. Elstner, D. Porezag, G. Jungnickel, J. Elsner, M. Haugk, et al., Self-consistent-charge density-functional tight-binding method for simulations of complex materials properties, Phys. Rev. B 58 (1998) 7260.
[58] G. Zheng, M. Lundberg, J. Jakowski, T. Vreven, M.J. Frisch, et al., Implementation and benchmark tests of the DFTB method and its application in the ONIOM method, Int. J. Quant. Chem. 109 (2009) 1841.
[59] S. Plimton, Fast parallel algorithms for short-range molecular dynamics, J. Comp. Phys. 117 (1995) 1−19.
[60] A.C.T. van Duin, S. Dasgupta, F. Lorant, W.A. Goddard III, ReaxFF: a reactive force field for hydrocarbons, J. Phys. Chem. A 105 (2001) 9396.
[61] M.R. Weismiller, A.C.T. van Duin, J. Lee, R.A. Yetter, ReaxFF reactive force field development and applications for molecular dynamics simulations of ammonia borane dehydrogenation and combustion, J. Phys. Chem. A 114 (2010) 5485.
[62] A. Strachan, A.C.T. van Duin, D. Chakraborty, S. Dasgupta, W.A. Goddard III, Shock waves in high-energy materials: the initial chemical events in nitramine RDX, Phys. Rev. Lett. 91 (2003) 098301.
[63] F.J. Domínguez-Gutiérrez, P.S. Krstić, Sputtering of lithiated and oxidated carbon surfaces by low-energy deuterium irradiation, J. Nucl. Mater. 492 (2017) 56.
[64] F.J. Domínguez-Gutiérrez, P.S. Krstić, Chemical sputtering of boronized and oxidized carbon surfaces irradiated by low-energy deuterium atoms, J. Appl. Phys. 212 (2017) 215302.
[65] M. Lucia, R. Kaita, R. Majeski, F. Bedoya, J.P. Allain, et al., Development progress of the materials analysis and particle probe, Sci. Instrum. 85 (2014) 11D835 [66a].
[66] C.N. Taylor, B. Heim, S. Gonderman, J.P. Allain, Z. Yang, et al., Materials analysis and particle probe: a compact diagnostic system for in situ analysis of plasma-facing components (invited), Rev. Sci. Instrum. 83 (2012) 10D703.

[67] M. Baldwin, R. Doerner, R. Causey, S. Luckhardt, R. Conn, Recombination of deuterium atoms on the surface of molten Li-LiD, J. Nucl. Mat. 306 (2002) 15−20.
[68] M. Baldwin, R. Doerner, S. Luckhardt, R. Conn, Deuterium retention in liquid lithium, Nucl. Fusion 42 (2002) 1318.
[69] J. Allain, D. Ruzic, Measurements and modelling of solid phase lithium sputtering, Nucl. Fusion 42 (2002) 202.
[70] W.R. Wampler, C.H. Skinner, H.W. Kugel, A.L. Roquemore, Measurement of lithium and deuterium on NSTX carbon tiles, J. Nucl. Mat. (2009) 1−4.
[71] J.H. Scofield, Theoretical Photoionization Cross Sections from 1 to 1500 KeV, Lawrence Livermore Lab. Rept. UCRL-51326, 1973.
[72] A. Allouche, P. Krstic, The effect of surface oxidation on atomic hydrogen adsorption on lithium-doped graphite surfaces, Carbon 50 (2012) 3882.
[73] A. Allouche, P.S. Krstic, Atomic hydrogen adsorption on lithium-doped graphite surfaces, Carbon 50 (2012) 510.
[74] C.N. Taylor, J.P. Allain, K.E. Luitjohan, P.S. Krstic, J. Dadras, et al., Differentiating the role of lithium and oxygen in retaining deuterium on lithiated graphite plasma-facing components, Phys. Plasma 21 (2014) 057101.
[75] J.P. Allain, C.N. Taylor, Lithium-based surfaces controlling fusion plasma behavior at the plasma-material interface, Phys. Plasma 19 (2012) 056126.
[76] A.L. Neff, J.P. Allain, F. Bedoya, T.W. Morgan, G. De Temmerman, High flux irradiations of Li coatings on polycrystalline W and ATJ graphite with D, He, and He-seeded D plasmas at Magnum PSI, J. Nucl. Mater. 463 (2015) 1147.
[77] J.P. Allain, M.D. Coventry, D.N. Ruzic, Collisional and thermal effects on liquid lithium sputtering, Phys. Rev. B 76 (2007) 205434.
[78] B. Dunweg, W. Paul, Brownian dynamics simulations without Gaussian random numbers, Int. J. Mod. Phys. C 02 (1991) 817.
[79] J.G. Buijnsters, R. Gago, I. Jiménez, M. Camero, F. Agulló-Rueda, et al., Hydrogen quantification in hydrogenated amorphous carbon films by infrared, Raman, and X-ray absorption near edge spectroscopies, J. Appl. Phys. 105 (2009) 093510.
[80] B. Heim, C.N. Taylor, D.M. Zigon, S. O'Dell, J.P. Allain, Deuterium ion−surface interactions of liquid-lithium thin films on micro-porous molybdenum substrates, Nucl. Instrum. Methods B 269 (2011) 1262.
[81] A.L. Neff, Dynamic Interactions Between Energetic D and He Ions on Lithium-Tungsten Plasma-Facing Interfaces, Doctoral thesis, University of Illinois at Urbana-Champaign, Urbana, IL, USA, 2017.